

ORIGINAL ARTICLE

Models for Machining Accuracy in Multi-Tool Adjustment

N.D. Yusubov¹ and H.M. Abbasova²

¹Department of Technology of Machine Building, Azerbaijan Technical University, 25 H. Cavid avenue, Baku, Azerbaijan AZ 1073
Phone: (+99450) 3245012; Fax: (+99412) 5383280

²Department of Technology of Machine Building, Azerbaijan Technical University, 25 H. Cavid avenue, Baku, Azerbaijan AZ 1073

ABSTRACT – The article discusses the technology capabilities of multi-purpose CNC machines, and possible options for implementing parallel multi-tool processing. It was revealed that the technological capabilities of these machines are used at best by 50% in factories. This is due to the lack of recommendations for the design and use of such adjustments for these machines. To this end, generalised lattice matrix models of the accuracy of multi-tool machining have been developed in order to fulfill the requirements of algorithmic uniformity models and their structural transparency. The use of lattice matrices greatly simplifies the error in model of multi-tool machining and makes it extremely visual. Also, full-factorial distortion models and scattering fields of the dimensions of multi-tool machining performed on modern multi-purpose CNC lathe machines have been developed to take into account the angular displacements of the workpiece when machining parts with prevailing overall dimensions. They take into account the flexibility of the technological system for all six degrees of freedom to identify the influence degree of complex of technological factors on the machining accuracy (structure of multi-tool adjustment, deformation properties of subsystems of a technological system, cutting conditions). A methodology has been developed for determining the complex characteristics of compliance of a technological system. On the basis of the developed accuracy models in spatial adjustments, it is possible to develop recommendations for the design of adjustments for modern multi-purpose machines in CNC turning group (creation of CAD of multi-tool machining). Thus, it is possible to achieve a number of ways to control multi-tool machining, including improving the structure of multi-tool adjustment, calculating the limiting cutting conditions.

ARTICLE HISTORY

Revised: 22nd June 2020

Accepted: 9th Sept 2020

KEYWORDS

*Models for machining accuracy,
Multi-tool machining,
Multi-purpose CNC machines,
Lattice matrix models of accuracy,
Full-factor models of accuracy*

INTRODUCTION

A promising direction in machine-building technology is the development of operations with the combination of several technological passes in time - multi-tool parallel machining, which is performed at the total (for different tools) spindle speed with the workpiece and the total machining time [1-2-3]. Multi-tool machining on multi-purpose CNC machines of the new generation is most effective. Multi-purpose machines that combine the capabilities of CNC lathes and machining centres are currently one of the fastest-growing metalworking concepts. The capabilities of the machine to carry out boring without changing tool holes, facing, internal and external grooving, facing on the backside of the workpiece, boring step holes on the inside of the workpiece, boring conical holes and holes of other shapes.

Program control of all movements of working bodies of the machine and automatic tool change with a large number of programmable coordinates allows the automated processing of the most complex case parts on all sides from one fastening, except for the surfaces on which the workpieces are based and fixed. This helps to achieve the highest accuracy of the relative positioning of the machined surfaces. It is known that in the conditions of production of parts in small quantities, the proportion of machining time, that is, time of direct metal cutting does not exceed 18-20% in the total time of the machining process on traditional machines with manual control. On numerically controlled machines this proportion increases to 45-50%, and on multi-operational machines, it reaches 70-75%. The dimensional stability of the parts obtained on multi-operational machines allows reducing the number of control operations by 50-70% [4-5]. Installation and fixing of the workpiece, as well as the removal of the part, are performed by manual labour.

As a result, the productivity of manufacturing parts on multi-purpose machines is 4 to 10 times higher than on universal ones. At the same time, the simplicity of adjustment and readjustment of multi-operational machines, as well as the elimination of complex and expensive technological equipment (templates, copiers, special devices) create conditions that allow the use of such machines in small-scale and pilot production, especially in the case of preparing control programs using computers.

Analysis of Modern Multi-Purpose CNC Machines For Multi-Tool Processing

The analysis of technological equipment presented on the market was carried out, on which the implementation of multi-tool machining is possible [1]. In the process of this analysis, five types of design of multi-purpose machines were

identified and for each type of structure machine models of representatives were selected. Having familiarised with the most common types of designs of multi-purpose machines, a detailed analysis of the capabilities of each type of equipment was carried out and possible adjustments on them were considered. In the course of the analysis, it turned out that the use of multi-tool machining in most plants is impossible due to the lack of equipment on which such machining could be performed. Some factories have equipment on which multi-tool machining is possible, but it is used for simultaneous machining of several parts (in the spindle and counter spindle), and not for simultaneous machining of several surfaces. Summing up, we can say that most enterprises do not have equipment on which parallel multi-tool machining is possible, and those few plants that have CNC multi-purpose machines use them at best for 50% of their technological capabilities. This situation has arisen due to the fact that there are no recommendations on the design and application of such adjustments [2].

Of course, there is a lot of research that characterises the multi-tool machining and technological capabilities of CNC multi-purpose machines [6-22]. The specific issues addressed in these studies ultimately do not provide the theoretical basis for the application and design of multi-tool adjustments. For example, [6-9] studies have focused on the nature of double-tool, double-carriage machining. But here, too, there is no question of complex matrix models, consisting of a model of the scattering area of the dimensions during the machining of workpiece sets and distortion of the accuracy of dimensions performed in multi-tool adjustments. There are no attempts to develop models based on the balance of force effects of the tools, taking into account the arbitrary spatial location of the tools in the adjustment in CNC machines during the design of multi-tool machining, if the working space of the machines allows.

The basis of the theory of design and optimisation of multi-tool machining, multi-tool adjustment based on force interaction of tools, were laid in works [23-24-25-26-27]. However, he considered only two classes of simple flat multi-tool adjustments when implementing them on automatic machines with cam control.

N.D. Yusubov, on the basis of the classification of multi-tool adjustments of modern automatic lathes, developed a set of matrix models of the accuracy of the dimensions to be performed, including models of distortion of dimensions and models of scattering fields of dimensions when processing a batch of workpieces, where the compliance of the technological system along all coordinate axes was taken into account for the first time, and arbitrary spatial arrangement of adjustment tools is allowed [23-24-25-26-27].

Matrix Models of Distortion for Performed Dimensions In Multi-Tool Two-Carriage Single-Coordinate Adjustments

In the models of the accuracy of dimensions [23-24-25-26] performed in multi-tool adjustment, the basis is elastic displacements of the vertices of the tool forming the executed dimension relative to the surface of the workpiece machined by it in the direction of the performed dimension. These elastic displacements are the result of the combined effect of cutting forces from all simultaneously working adjustment tools and the ultimate compliance of the elements of the technological system that perceive this force. For multi-tool machining, especially turning, on modern multi-tool machines, it is characteristic that complicated spatial arrangement of cutting tools that work simultaneously and placed several pieces on one, two or even three carriages. Therefore, in multi-tool machining, the system of forces acting on the elements of the technological system is a spatial general form.

The elastic displacement of an element of a technological system is a vector, the direction and magnitude of which are determined by the resulting vector of forces acting on this element, and the ratio of its compliance over possible degrees of freedom. Therefore, the description of distortion equations of the dimensions performed in multi-tool adjustment in vector form is natural. Since the full characteristic of the compliance of an element of the technological system for all possible degrees of freedom is described by a matrix, we come to the matrix form of models of machining accuracy.

As a rule, in multi-tool adjustments, own compliance of cutting tools is minimised. This is achieved either by selecting the appropriate design parameters of the tools or by using special fixtures and holders. Therefore, the movement of the tool vertices is ensured, as in the case of one-tool adjustment [28], due to the deformation of the entire block of elements of the technological system: carriage - holder - tool. For a multi-tool two-carriage adjustment, the analytical problem is reduced to the interaction of a 3-body system. To identify the main features of the effect of the double carriage during multi-tool machining, we consider the simplest multi-tool adjustment: on the longitudinal carriage, there is one turning cutting tool, on the cross carriage one facing tool (Figure 1). Here the technological system is decomposed into the following three subsystems: "workpiece-chuck-spindle" - subsystem 0; "Cutter-holder-longitudinal carriage" subsystem 1; "Cutter-holder-cross carriage" - subsystem 2. The performed decomposition is based on the assumption that all tools have sufficient rigidity and that deformations in the technological system can be considered at the subsystem level. It should be noted that a large number of tools on the carriage leads to a system of acting forces, which can be replaced by the resultant force. Therefore, the restriction in the form of one tool on each carriage does not in the least reduce the generality of the statement and consideration of the problem, while at the same time making the calculation scheme more transparent. Even for the case when each carriage has one tool, the scheme of applying forces deforming the system under consideration is significantly complicated. In this case, we have two systems of forces - the impact from the tools of each carriage (see. Figure 1). Both systems of forces are spatial. In Figure 1 the reaction force P_{z_2} from the impact of the tools of the cross carriage is directed upwards. The reaction force P_{z_1} from the impact of the tools of the longitudinal carriage is directed downward. Similarly, P_{y_1} which forms force \mathbf{P}_1 and P_{y_2} which forms force \mathbf{P}_2 are directed against each other. Here, cutting force vectors \mathbf{P}_1 and \mathbf{P}_2 can be written as $\mathbf{P}_1 = \{P_{x1}; P_{y1}; P_{z1}\}$ and $\mathbf{P}_2 = \{P_{x2}; -P_{y2}; -P_{z2}\}$ according to the layout.

Here, g_1, g_2 is the displacement of the contact point for each pair of contacting bodies, respectively for bodies 1 and 2; P_0^1 - the reaction force of the P_1 of body 1 to body 0, thus, the action of body 0 on body 1; P_0^2 - the reaction force of the P_2 of body 2 to body 0, thus, the action of body 0 on body 2; e_0 - compliance characteristic of body 0, thus, $e_0 = \begin{pmatrix} e_{xx}^0 & e_{xy}^0 & e_{xz}^0 \\ e_{yx}^0 & e_{yy}^0 & e_{yz}^0 \\ e_{zx}^0 & e_{zy}^0 & e_{zz}^0 \end{pmatrix}$, where, e_{xx}^0 is a movement in the direction of the X axis from the unit force P_x , e_{xy}^0 is a movement in the direction of the X axis from the unit force P_y , e_{xz}^0 is a movement in the direction of the X axis from the unit force P_z ; e_{yx}^0 is a movement in the direction of the Y axis from the unit force P_x , e_{yy}^0 is a movement in the direction of the Y axis from the unit force P_y , e_{yz}^0 is a movement in the direction of the Y axis from the unit force P_z ; e_{zx}^0 is a movement in the direction of the Z axis from the unit force P_x , e_{zy}^0 is a movement in the direction of the Z axis from the unit force P_y , e_{zz}^0 is a movement in the direction of the Z axis from the unit force P_z ; e_{01}, e_{02} - are combined compliance matrices for two groups of technological subsystems: $e_{01} = e_0 + e_1$; $e_{02} = e_0 + e_2$, where, e_1 - is compliance characteristic of body 1; e_2 - is compliance characteristic of body 2.

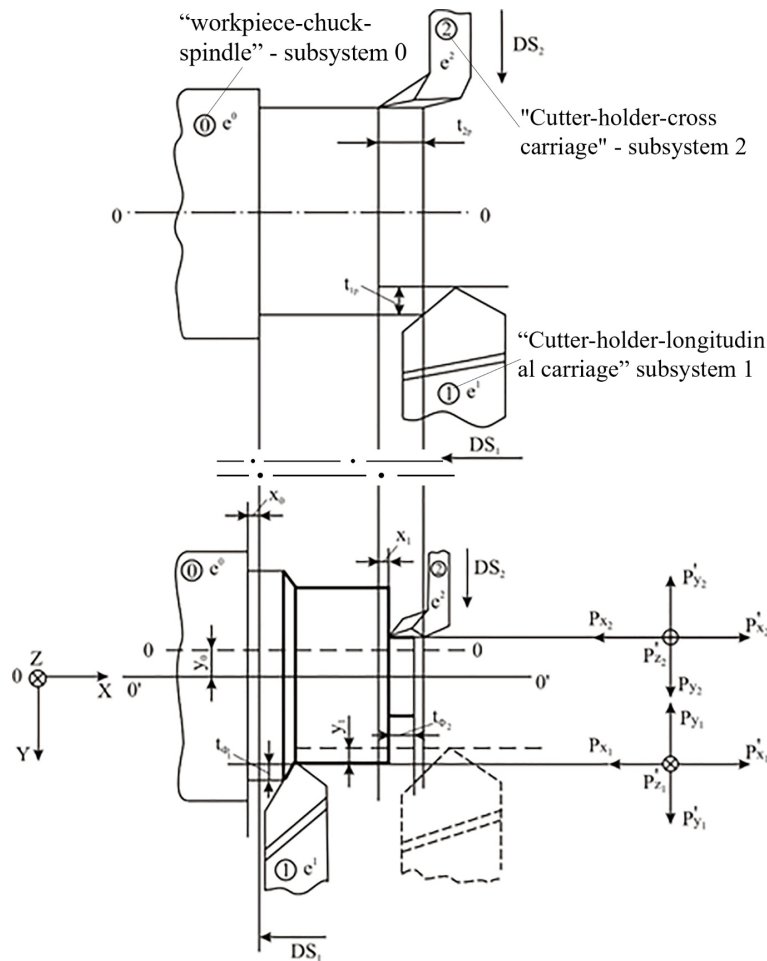


Figure 1. Design scheme of the elastic displacements of technological subsystems during multi-tool two-carriage machining.

Then the equation of the displacement of the contact point for each pair of contacted bodies g_1 and g_2 according to [23-25] in the expanded form is presented as:

$$g_1 = \begin{pmatrix} g_{1x} \\ g_{1y} \\ g_{1z} \end{pmatrix} = \begin{pmatrix} e_{xx}^{01} & e_{xy}^{01} & e_{xz}^{01} \\ e_{yx}^{01} & e_{yy}^{01} & e_{yz}^{01} \\ e_{zx}^{01} & e_{zy}^{01} & e_{zz}^{01} \end{pmatrix} \begin{pmatrix} P_{x1} \\ P_{y1} \\ P_{z1} \end{pmatrix} + \begin{pmatrix} e_{xx}^0 & e_{xy}^0 & e_{xz}^0 \\ e_{yx}^0 & e_{yy}^0 & e_{yz}^0 \\ e_{zx}^0 & e_{zy}^0 & e_{zz}^0 \end{pmatrix} \begin{pmatrix} P_{x2} \\ -P_{y2} \\ -P_{z2} \end{pmatrix} \quad (1)$$

$$g_2 = \begin{pmatrix} g_{2x} \\ g_{2y} \\ g_{2z} \end{pmatrix} = \begin{pmatrix} e_{xx}^{02} & e_{xy}^{02} & e_{xz}^{02} \\ e_{yx}^{02} & e_{yy}^{02} & e_{yz}^{02} \\ e_{zx}^{02} & e_{zy}^{02} & e_{zz}^{02} \end{pmatrix} \begin{pmatrix} P_{x2} \\ -P_{y2} \\ -P_{z2} \end{pmatrix} + \begin{pmatrix} e_{xx}^0 & e_{xy}^0 & e_{xz}^0 \\ e_{yx}^0 & e_{yy}^0 & e_{yz}^0 \\ e_{zx}^0 & e_{zy}^0 & e_{zz}^0 \end{pmatrix} \begin{pmatrix} P_{x1} \\ P_{y1} \\ P_{z1} \end{pmatrix} \quad (2)$$

From Eq.(1), for the dimension distortion along Y axis, that is, the diametric dimensions formed from the longitudinal carriage, we obtain from consideration of the second component of the g_1 :

$$g_{1y} = e_{yx}^{01}P_{x1} + e_{yy}^{01}P_{y1} + e_{yz}^{01}P_{z1} + e_{yx}^0P_{x2} - e_{yy}^0P_{y2} - e_{yz}^0P_{z2} \tag{3}$$

From (2) for linear dimensions (along the X axis) formed from the cross carriage, we obtain:

$$g_{2x} = e_{xx}^{02}P_{x2} - e_{xy}^{02}P_{y2} - e_{xz}^{02}P_{z2} + e_{xx}^0P_{x1} + e_{xy}^0P_{y1} + e_{xz}^0P_{z1} \tag{4}$$

Expression (1) and (2) are generalised matrix models of machining errors in the multi-tool two-carriage adjustment shown in Figure 1.

Thus, model (1) and (2) are matrix models of distortion of shapes and dimensions formed in the multi-tool two-carriage adjustment shown in Figure 1. As we can see, dimension distortions during two-carriage machining depend on all tools of the adjustment. So, the distortion of the diametric dimension g_{y1} performed from the longitudinal support is influenced not only by the cutting depth t_1 , feed S_1 , and other cutting conditions $(C_{P_{y1}}, x_{p_{y1}}, y_{p_{y1}})$ of the turning cutter directly forming this dimension, but also by t_2, S_2 and others cutting conditions $(C_{P_{y2}}, x_{p_{y2}}, y_{p_{y2}})$ of a cutting tool standing on a cross carriage and machining a completely different surface. The situation is similar for the distortion of the linear dimension performed from the cross carriage. Model (1) and (2) allow us to calculate the distortion of the diametric dimensions performed from the longitudinal carriage, and linear, performed from the cross carriage, in multi-tool two-carriage machining. They can be used in the calculation of tuning dimensions.

LATTICE MATRIX MODELS OF THE ACCURACY OF MULTI-TOOL MACHINING

In accordance with the provisions of the matrix theory of machining accuracy for the simplest two-carriage adjustment [23-25] - the right turning cutter on the longitudinal carriage and the left facing cutter on the cross-carriage opposite to the longitudinal - we have the following two matrix equations:

$$g_1 = e_{01}P_1 + e_0P_2 \tag{5}$$

$$g_2 = e_{02}P_2 + e_0P_1 \tag{6}$$

Where, g_1 and g_2 are the vectors of elastic displacements relative to the machined surface of the vertices of the turning and facing tools, respectively;

P_1 and P_2 are the cutting force vectors on the longitudinal and cross carriages, respectively;

e_0 - the compliance matrix of the subsystem workpiece - spindle;

e_{01} and e_{02} - matrices of the total compliance of the complexes of the subsystems longitudinal carriage - turning cutter - workpiece - spindle and cross carriage - facing tool - workpiece - spindle, respectively;

$$e_{01} = \begin{pmatrix} e_{xx}^{01} & e_{xy}^{01} & e_{xz}^{01} \\ e_{yx}^{01} & e_{yy}^{01} & e_{yz}^{01} \\ e_{zx}^{01} & e_{zy}^{01} & e_{zz}^{01} \end{pmatrix} \tag{7}$$

$$e_{02} = \begin{pmatrix} e_{xx}^{02} & e_{xy}^{02} & e_{xz}^{02} \\ e_{yx}^{02} & e_{yy}^{02} & e_{yz}^{02} \\ e_{zx}^{02} & e_{zy}^{02} & e_{zz}^{02} \end{pmatrix} \tag{8}$$

The setting, in accordance with the theory of cutting, the coordinate components of the cutting forces in the coordinate system of the machine, we transform Eq. (5) and (6) to the form:

$$g_1 = e_{01} \begin{pmatrix} P_x^1 \\ P_y^1 \\ P_z^1 \end{pmatrix} + e_0 \begin{pmatrix} P_x^2 \\ -P_y^2 \\ -P_z^2 \end{pmatrix} \tag{9}$$

$$g_2 = e_{02} \begin{pmatrix} P_x^2 \\ -P_y^2 \\ -P_z^2 \end{pmatrix} + e_0 \begin{pmatrix} P_x^1 \\ P_y^1 \\ P_z^1 \end{pmatrix} \tag{10}$$

where, the lower indices of the constituent cutting forces indicate the coordinate axis, and the upper ones are the carriage number.

From the matrix in Eq. (9) and (10) we obtain the expressions for the relative elastic displacements of the vertices of the cutters in all coordinate directions:

$$g_x^1 = e_{xx}^{01}P_x^1 + e_{xy}^{01}P_y^1 + e_{xz}^{01}P_z^1 + e_{xx}^0P_x^2 - e_{xy}^0P_y^2 - e_{xz}^0P_z^2 \tag{11}$$

$$g_y^1 = e_{yx}^{01}P_x^1 + e_{yy}^{01}P_y^1 + e_{yz}^{01}P_z^1 + e_{yx}^0P_x^2 - e_{yy}^0P_y^2 - e_{yz}^0P_z^2 \tag{12}$$

$$g_z^1 = e_{zx}^{01}P_x^1 + e_{zy}^{01}P_y^1 + e_{zz}^{01}P_z^1 + e_{zx}^0P_x^2 - e_{zy}^0P_y^2 - e_{zz}^0P_z^2 \tag{13}$$

$$g_x^2 = e_{xx}^0P_x^1 + e_{xy}^0P_y^1 + e_{xz}^0P_z^1 + e_{xx}^{02}P_x^2 - e_{xy}^{02}P_y^2 - e_{xz}^{02}P_z^2 \tag{14}$$

$$g_y^2 = e_{yx}^0P_x^1 + e_{yy}^0P_y^1 + e_{yz}^0P_z^1 + e_{yx}^{02}P_x^2 - e_{yy}^{02}P_y^2 - e_{yz}^{02}P_z^2 \tag{15}$$

$$g_z^2 = e_{zx}^0P_x^1 + e_{zy}^0P_y^1 + e_{zz}^0P_z^1 + e_{zx}^{02}P_x^2 - e_{zy}^{02}P_y^2 - e_{zz}^{02}P_z^2 \tag{16}$$

Here, the first three expression, (11) to (13) describe the relative elastic displacements of the turning tool, and expression (14) to (16) describe the facing tool. Moreover, only two of them are important for technology and controlled:

- g_y^1 - is the distortion of the diametric dimension formed from the longitudinal carriage with turning cutter;
- g_x^2 - is the distortion of the linear dimension formed from the cross carriage with a facing cutter.

The scalar Eq. (12) and (14), even for the simplest considered adjustment, are quite complicated for analysis. Therefore, the matrix theory of accuracy is initially focused on the use of computer technology. In this case, the requirements of algorithmic uniformity of models and their structural transparency come first.

To ensure algorithmic uniformity, it is proposed that the set of scalar Eq. (11) to (15) be presented in matrix form in six-dimensional hyperspace:

$$\begin{pmatrix} g_x^1 \\ g_y^1 \\ g_z^1 \\ g_x^2 \\ g_y^2 \\ g_z^2 \end{pmatrix} = \begin{pmatrix} e_{xx}^{01} & e_{xy}^{01} & e_{xz}^{01} & e_{xx}^0 & e_{xy}^0 & e_{xz}^0 \\ e_{yx}^{01} & e_{yy}^{01} & e_{yz}^{01} & e_{yx}^0 & e_{yy}^0 & e_{yz}^0 \\ e_{zx}^{01} & e_{zy}^{01} & e_{zz}^{01} & e_{zx}^0 & e_{zy}^0 & e_{zz}^0 \\ e_{xx}^0 & e_{xy}^0 & e_{xz}^0 & e_{xx}^{02} & e_{xy}^{02} & e_{xz}^{02} \\ e_{yx}^0 & e_{yy}^0 & e_{yz}^0 & e_{yx}^{02} & e_{yy}^{02} & e_{yz}^{02} \\ e_{zx}^0 & e_{zy}^0 & e_{zz}^0 & e_{zx}^{02} & e_{zy}^{02} & e_{zz}^{02} \end{pmatrix} \begin{pmatrix} P_x^1 \\ P_y^1 \\ P_z^1 \\ P_x^2 \\ -P_y^2 \\ -P_z^2 \end{pmatrix} \tag{17}$$

Here the vector on the left side of the equation describes all coordinate movements of the points in question; the vector on the right side describes the force loading scheme of technological subsystems; the matrix characterises the compliance of the participating technological subsystems. It is easy to see that the multiplication of the matrix and the vector on the right side of Eq. (17) gives all scalar Eq. (11) to (16).

Thus, Eq. (17) in its simplest form, is a generalised matrix equation for the machining error describing the whole complex of dimension distortions performed in a two-carriage two-tool adjustment. Equation (17) is algorithmically elementary, but not very obvious. To ensure the clarity of the generalised matrix equation of machining error (17), it is proposed to use the apparatus of lattice matrices [23].

Having selected the matrix in Eq. (17) the blocks of elements that have an independent technological meaning, we come to the lattice-matrix model in which the elements of the matrices themselves are matrices and, accordingly, the elements of vectors are vectors:

$$\begin{pmatrix} g_1 \\ g_2 \end{pmatrix} = \begin{pmatrix} e_{01} & e_0 \\ e_0 & e_{02} \end{pmatrix} \begin{pmatrix} P_1 \\ P_2 \end{pmatrix} \tag{18}$$

A block of the first three components of the displacement vector in Eq. (17) formed a vector - the first component of the block displacement vector in the lattice-matrix model (18). The second three components of the displacement vector in Eq. (17) formed a vector - the second component of the block displacement vector in equation (18). As a result, the block displacement vector has two components - the displacement vector on the longitudinal carriage and the displacement vector on the cross carriage, that is, it has an extremely transparent structure. The situation with the description of the force load is similar. By combining the coordinate components of the forces of the longitudinal and cross carriages, respectively, the six-component load vector of Eq. (17) was transformed into a two-component block vector of Eq. (18), where each component is the force vector of the corresponding carriage. Also, in the sixth-order compliance matrix, four semantic blocks are identified that correspond to the compliance matrices of the selected technological subsystems (7) to (8).

Obviously, from the lattice-matrix model (18) by multiplying the block compliance matrix by the block load vector, we obtain the well-known matrix equations of dimension distortion for each carriage (5)-(6). So, the use of lattice matrices greatly simplifies the error model of multi-tool machining and makes it extremely visual. However, the lattice compliance matrix contains the constituent elements — the e_{01} and e_{02} matrices, which characterise the total compliance of the complex of two subsystems. It is more practical to operate with the own characteristics of technological subsystems – e_1 and e_2 . From the theory of matrices, we get the relation:

$$\begin{pmatrix} e_{01} & e_0 \\ e_0 & e_{02} \end{pmatrix} = \begin{pmatrix} e_0 + e_1 & e_0 \\ e_0 & e_0 + e_2 \end{pmatrix} = e_0K + \begin{pmatrix} e_1 & 0 \\ 0 & e_2 \end{pmatrix} \tag{19}$$

where $K = \begin{pmatrix} 1 & 1 \\ 1 & 1 \end{pmatrix}$ is the square matrix of the corresponding order. Taking into account the relation (19), the lattice-matrix model is reduced to the canonical form:

$$\begin{pmatrix} g_1 \\ g_2 \end{pmatrix} = e_0 K \begin{pmatrix} P_1 \\ P_2 \end{pmatrix} + \begin{pmatrix} e_1 & 0 \\ 0 & e_2 \end{pmatrix} \begin{pmatrix} P_1 \\ P_2 \end{pmatrix} \tag{20}$$

Here, the first term characterises the contribution to the error of the two-tool two-carriage machining of the entire complex of cutting forces through the compliance of the spindle, the second - through the compliance of the carriages. Let us consider how the proposed scheme for converting traditional matrix models of machining errors into block-matrix ones is implemented using examples of multi-tool adjustments.

Adjustment 2 - three carriages, one tool on each carriage. Decomposition of the technological system into four subsystems is natural: spindle and carriages. For each subsystem, a compliance matrix is specified: e_0, e_1, e_2, e_3 . In accordance with the matrix theory of accuracy, by analogy with (5 - 6), we obtain the expressions for the dimension distortion vectors on each carriage:

$$g_1 = (e_0 + e_1)P_1 + e_0(P_2 + P_3) \tag{21}$$

$$g_2 = (e_0 + e_2)P_2 + e_0(P_1 + P_3) \tag{22}$$

$$g_3 = (e_0 + e_3)P_3 + e_0(P_1 + P_2) \tag{23}$$

Turning to hyperspace (9-dimensional) and forming blocks in matrices, we obtain, by analogy with (18), the lattice-matrix model:

$$\begin{pmatrix} g_1 \\ g_2 \\ g_3 \end{pmatrix} = \begin{pmatrix} e_0 + e_1 & e_0 & e_0 \\ e_0 & e_0 + e_2 & e_0 \\ e_0 & e_0 & e_0 + e_3 \end{pmatrix} \begin{pmatrix} P_1 \\ P_2 \\ P_3 \end{pmatrix} \tag{24}$$

which is reduced to the canonical form:

$$\begin{pmatrix} g_1 \\ g_2 \\ g_3 \end{pmatrix} = e_0 K \begin{pmatrix} P_1 \\ P_2 \\ P_3 \end{pmatrix} + \begin{pmatrix} e_1 & 0 & 0 \\ 0 & e_2 & 0 \\ 0 & 0 & e_3 \end{pmatrix} \begin{pmatrix} P_1 \\ P_2 \\ P_3 \end{pmatrix} \tag{25}$$

The structural identity of Eq. (20) and Eq. (25) is obvious. Adjustment 3 - two tools on one carriage. Here, decomposition into two subsystems is sufficient: spindle and carriage with ductility matrices e_0, e_1 . In accordance with the matrix theory of accuracy, we obtain the simplest matrix equation:

$$g = (e_0 + e_1)(P_1 + P_2) \tag{26}$$

where P_1 and P_2 are the cutting force vectors from each tool.

Adjustment 4 - two tools on the same carriage, but the tools are non-rigid. In this case, the decomposition of the technological system into four subsystems is required: spindle, carriage and each tool. For the selected subsystems, we set the compliance matrices: e_0, e_c, e_1, e_2 . Unlike the previous case, here, each tool gives its distortion to the executed dimension. In accordance with the matrix theory of accuracy of expression for distortion vectors on each tool:

$$g_1 = (e_0 + e_c + e_1)P_1 + (e_0 + e_c)P_2 \tag{27}$$

$$g_2 = (e_0 + e_c + e_2)P_1 + (e_0 + e_c)P_2 \tag{28}$$

Acting by analogy with adjustment 1 and adjustment 2, we get the lattice-matrix model:

$$\begin{pmatrix} g_1 \\ g_2 \end{pmatrix} = \begin{pmatrix} e_0 + e_c + e_1 & e_0 + e_c \\ e_0 + e_c & e_0 + e_c + e_2 \end{pmatrix} \begin{pmatrix} P_1 \\ P_2 \end{pmatrix} \tag{29}$$

which also converts to canonical form:

$$\begin{pmatrix} g_1 \\ g_2 \end{pmatrix} = (e_0 + e_c)K \begin{pmatrix} P_1 \\ P_2 \end{pmatrix} + \begin{pmatrix} e_1 & 0 \\ 0 & e_2 \end{pmatrix} \begin{pmatrix} P_1 \\ P_2 \end{pmatrix} \tag{30}$$

Here, as in model (21) and (25), the first term characterises the contribution to the error of compliance of the subsystems common for the dimensions being formed, the second term is the individual contribution of each tool to its size.

Adjustment 5 - two carriages, one tool on each carriage, non-rigid tools. Here, decomposition into five subsystems is necessary: a spindle, two carriages, two tools, with the corresponding ductility matrices: $e_0, e_{c1}, e_{c2}, e_1, e_2$. In accordance with the matrix theory of accuracy, for each tool, we obtain two distortion vectors of the performed dimensions:

$$g_1 = (e_0 + e_{c1} + e_1)P_1 + e_0P_2 \tag{31}$$

$$g_2 = (e_0 + e_{c2} + e_2)P_2 + e_0P_1 \tag{32}$$

Forming, by analogy with Eq. (17), the combined matrix equation in 6-dimensional hyperspace and highlighting semantic blocks, we obtain a lattice-matrix model:

$$\begin{pmatrix} g_1 \\ g_2 \end{pmatrix} = \begin{pmatrix} e_0 + e_{c1} + e_1 & e_0 \\ e_0 & e_0 + e_{c2} + e_2 \end{pmatrix} \begin{pmatrix} P_1 \\ P_2 \end{pmatrix} \tag{33}$$

In a canonical form, this model has three terms:

$$\begin{pmatrix} g_1 \\ g_2 \end{pmatrix} = e_0K \begin{pmatrix} P_1 \\ P_2 \end{pmatrix} + \begin{pmatrix} e_{c1} & 0 \\ 0 & e_{c2} \end{pmatrix} \begin{pmatrix} P_1 \\ P_2 \end{pmatrix} + \begin{pmatrix} e_1 & 0 \\ 0 & e_2 \end{pmatrix} \begin{pmatrix} P_1 \\ P_2 \end{pmatrix} \tag{34}$$

Each reflects its peculiarity of the formation of machining errors. The first term characterises the contribution of the ductility of the technological subsystem, which is the same for all carriages and tools - Spindle and the whole complex of cutting forces. The second term characterises the contribution of the ductility of the carriage, on which the executed dimension is formed, and the cutting forces acting on this carriage. The third term is the contribution of the compliance of the actual tool that forms this dimension.

Adjustment 6 - two carriages, two tools on each carriage, non-rigid tools. Here decomposition is already necessary for seven subsystems: spindle, two carriages, four tools. For each of the subsystems, a compliance matrix is defined: $e_0, e_{c1}, e_{11}, e_{12}, e_{c2}, e_{21}, e_{22}$. In tool ductility matrices, the first index specifies the carriage number; the second specifies the tool number on this carriage. Matrix models of dimension distortion vectors for each of the tools have the form:

$$g_{11} = (e_0 + e_{c1} + e_{11})P_{11} + (e_0 + e_{c1})P_{12} + e_0(P_{21} + P_{22}) \tag{35}$$

$$g_{12} = (e_0 + e_{c1} + e_{12})P_{12} + (e_0 + e_{c1})P_{11} + e_0(P_{21} + P_{22}) \tag{36}$$

$$g_{21} = (e_0 + e_{c2} + e_{21})P_{21} + (e_0 + e_{c2})P_{22} + e_0(P_{11} + P_{12}) \tag{37}$$

$$g_{22} = (e_0 + e_{c2} + e_{22})P_{22} + (e_0 + e_{c2})P_{21} + e_0(P_{11} + P_{12}) \tag{38}$$

In accordance with the proposed approach (the combined matrix model in 12-dimensional hyperspace, the allocation of semantic blocks), we obtain the lattice-matrix model:

$$\begin{pmatrix} g_{11} \\ g_{12} \\ g_{21} \\ g_{22} \end{pmatrix} = \begin{pmatrix} e_0 + e_{c1} + e_{11} & e_0 + e_{c1} & e_0 & e_0 \\ e_0 + e_{c1} & e_0 + e_{c1} + e_{12} & e_0 & e_0 \\ e_0 & e_0 & e_0 + e_{c2} + e_{21} & e_0 + e_{c2} \\ e_0 & e_0 & e_0 + e_{c2} & e_0 + e_{c2} + e_{22} \end{pmatrix} \begin{pmatrix} P_{11} \\ P_{12} \\ P_{21} \\ P_{22} \end{pmatrix} \tag{39}$$

In a canonical form, this model also has three terms, each of which reflects its own mechanism for generating errors:

$$\begin{pmatrix} g_{11} \\ g_{12} \\ g_{21} \\ g_{22} \end{pmatrix} = e_0K \begin{pmatrix} P_{11} \\ P_{12} \\ P_{21} \\ P_{22} \end{pmatrix} + \begin{pmatrix} e_{c1} & e_{c1} & 0 & 0 \\ e_{c1} & e_{c1} & 0 & 0 \\ 0 & 0 & e_{c2} & e_{c2} \\ 0 & 0 & e_{c2} & e_{c2} \end{pmatrix} \begin{pmatrix} P_{11} \\ P_{12} \\ P_{21} \\ P_{22} \end{pmatrix} + \begin{pmatrix} e_{11} & 0 & 0 & 0 \\ 0 & e_{12} & 0 & 0 \\ 0 & 0 & e_{21} & 0 \\ 0 & 0 & 0 & e_{22} \end{pmatrix} \begin{pmatrix} P_{11} \\ P_{12} \\ P_{21} \\ P_{22} \end{pmatrix} \tag{40}$$

Thus, the use of lattice matrices allows to lead the model of machining accuracy for different types of multi-tool adjustments to the simplest form from the standpoint of algorithmic (24), (29), (33), (39).

The canonical lattice-matrix model (25), (30), (34), (40) is more transparent from the standpoint of the mechanism of formation of machining error in a multi-carriage multi-tool setup. The first term in it reflects the influence of the common subsystem for all tools - the spindle. The following describes the influence of the second-level subsystems - carriages, which in turn are common subsystems for carriage tools. And the third term reflects the influence of the tools that form the executed dimensions. The degree of influence of each subsystem is determined by its compliance, which is determined by the corresponding matrix. Tool compliance matrices of tools are arranged in a diagonal lattice matrix of tools. Carriage compliance matrices form a lattice-diagonal block carriage matrix. Obviously, for the case of absolute rigidity of any of the subsystems, the corresponding matrix degenerates into zero. Therefore, model (40) can be considered a generalised lattice-matrix model of machining accuracy for a multi-carriage multi-tool adjustment.

Full-Factor Model - Distortion of Executed Dimensions in Multi-Tool Two-Carriage Machining

The machining error models generated in Eq. (23)-(25) take into account only plane-parallel displacements of the subsystems of the technological system along the coordinate axes of the Cartesian coordinate system X, Y, Z. Such an approach to modelling the process of formation of machining errors is permissible for parts having overall dimensions of the same order in all coordinate directions.

However, in practice, it is not uncommon for parts to be machined with overall dimensions significantly different in different directions. For example, long shafts (predominant linear size), discs and flanges (predominant diametric size). In these cases, a significant contribution to the machining error can be made by turns of the workpiece, especially in the directions of the prevailing overall dimensions. The need to take into account angular displacements of workpiece under the action of cutting forces was indicated in [3, 29-42]. They even proposed the simplest analytical relationships for calculating these angular displacements.

However, all these dependencies are private, including a number of parameters, the determination of which in practice is fraught with insurmountable difficulties. For example, the centre of rotation of the spindle is generally a virtual object that cannot be practically measured. Most importantly, these models do not agree with the general laws of mechanics of elastically deformable systems. Therefore, they cannot be used to construct a unified theory of machining accuracy when taking into account the possible angular displacements of the subsystems of the technological system.

Considering a three-body system (as applied to two-carriage adjustments) with 6 degrees of freedom for each body and introducing compliance characteristics for each degree of freedom, the plane-parallel model of elastic displacements [23-24] is transformed into a full-factorial one:

$$w_1 = [e_{01} - (a_{0_1}^1 \xi_1 a_{0_1}^1 + a_{0_0}^0 \xi_0 a_{0_0}^0)]P^1 + [e_0 - a_{0_0}^0 \xi_0 a_{0_0}^0]P^2 \tag{41}$$

$$w_2 = [e_{02} - (a_{0_2}^2 \xi_2 a_{0_2}^2 + a_{0_0}^0 \xi_0 a_{0_0}^0)]P^2 + [e_0 - a_{0_0}^0 \xi_0 a_{0_0}^0]P^1 \tag{42}$$

Here: e_0 and ξ_0 are the matrices of plane-parallel and angular compliance of body 0, respectively ($\xi_0 = \begin{pmatrix} \xi_{0xx} & \xi_{0xy} & \xi_{0xz} \\ \xi_{0yx} & \xi_{0yy} & \xi_{0yz} \\ \xi_{0zx} & \xi_{0yz} & \xi_{0zz} \end{pmatrix}$); e_{01} and e_{02} are the total matrices of plane-parallel compliance of the contacting bodies (subsystems O_1 and O_2); ξ_0, ξ_1 and ξ_2 are the matrices of the angular compliance for contacting bodies; P^1 and P^2 are vector of forces applied respectively to body 1 and 2; $a_{0_0}^0, a_{0_1}^1$ and $a_{0_2}^2$ are matrices defining coordinating vectors of the point of application of the P^1 and P^2 forces relative to the base points of O_0, O_1 and O_2 , around which angular movements of the contacting bodies are carried out. A_1 and A_2 are the points of application of force P^1 and P^2 respectively; w_1 and w_2 - size distortions taking into account both plane-parallel and angular displacements.

Full-Factor Matrix Models Of Scattering Fields Of Executive Dimensions In Multi-Tool Two-Support Adjustments

Considering a three-body system (as applied to two-carriage adjustments) with 6 degrees of freedom for each body and introducing compliance characteristics for each degree of freedom, the plane-parallel model of elastic displacements is transformed into a full-factor one. By the nature of the force interaction, Yusubov identified two limiting cases of multi-tool adjustments [23-24]: opposed and non-opposed. In the opposing adjustment, all the cutting forces of one carriage are directed against the corresponding cutting forces of the other carriage. Such adjustments are traditional for turning-turret and turning multi-spindle automatic machines with cam control. In non-opposed adjustment, all the corresponding components of the cutting forces of both carriages are directed in the same direction. On modern CNC lathe machines, both types of adjustments are equally used.

The mechanism of the formation of the scattering field in a two-carriage opposed adjustment is more complicated than with single-adjustment machining. The dispersion of the rigidity of the technological system $j_F \in j_N \left[1 - \frac{\varepsilon}{2}; 1 + \frac{\varepsilon}{2} \right]$ and the strength properties of the workpiece material $C_F \in C_N \left[1 - \frac{\nu}{2}; 1 + \frac{\nu}{2} \right]$ determine the scale of the interval of dispersion of distortions in the dimensions of w_1 and w_2 . The influence of fluctuations of allowances $t_F \in \left[t - \frac{\Delta t}{2t + \frac{\Delta t}{2}} \right]$ on the carriages is ambiguous. Since the cutting forces on the longitudinal and cross carriages are directed against each other, fluctuations in the allowances Δt_1 and Δt_2 can also lead to a change in the balance of forces. As a result of this, the scattering intervals of the performed dimensions have three layout options.

Option I is characterised by the predominant influence of the longitudinal carriage, i.e. displacements from the action of the forces of the longitudinal carriage are so much more displacements from the forces of the cross carriage that the entire interval of dispersion of distortions is located on the positive axis: $w_{min_{max}}$. Option II is characterised by the predominant influence of the cross carriage, i.e. displacements from the action of the forces of the cross carriage are so much greater than displacements from the forces of the longitudinal carriage that the entire interval of scattering of distortions is located on the negative axis: $w_{min_{max}}$. Option III is characterised by a balanced effect of the longitudinal and cross carriages. The nominal distortion of the performed size is located in the vicinity of zero, and the interval of dispersion of distortions includes the origin: $w_{min_{max}}$.

The orientation of the scattering field relative to the nominal value is determined by the ratio of cutting depths on the carriages. So in option I, the allowance on the longitudinal carriage is maximum, and on the cross - minimum. The maximum value of the scattering interval is achieved with a maximum strength of the workpiece material and maximum flexibility of the technological system.

The analysis results from all options of the scattering field location and taking into account the known methodology for determining the scattering area [23-26], a unified model of the scattering field of dimensions is formed, which is performed from the longitudinal carriage in a two-carriage opposed adjustment.

$$\Delta w_1 = \left\{ \begin{array}{l} e_{01}t_1\mathbf{p}_t^1 - e_0t_2\mathbf{p}_t^2 + (-a_{0_1}^1\xi_1a_{0_1}^1 + a_{0_0}^0\xi_0a_{0_0}^0)t_1\mathbf{p}_t^1 + a_{0_0}^0\xi_0a_{0_0}^0t_2\mathbf{p}_t^2 \leq \\ \leq -\frac{e_{01}\Delta t_1\mathbf{p}_{\Delta t}^1 + e_0\Delta t_2\mathbf{p}_{\Delta t}^2}{2} + \frac{-(a_{0_1}^1\xi_1a_{0_1}^1 + a_{0_0}^0\xi_0a_{0_0}^0)\Delta t_1\mathbf{p}_{\Delta t}^1 - a_{0_0}^0\xi_0a_{0_0}^0\Delta t_2\mathbf{p}_{\Delta t}^2}{2} \quad \text{when} \\ \omega[e_{01}t_1\mathbf{p}_t^1 - e_0t_2\mathbf{p}_t^2] + [e_{01}\Delta t_1\mathbf{p}_{\Delta t}^1 + e_0\Delta t_2\mathbf{p}_{\Delta t}^2] + \omega[-(a_{0_1}^1\xi_1a_{0_1}^1 + a_{0_0}^0\xi_0a_{0_0}^0)t_1\mathbf{p}_t^1 + a_{0_0}^0\xi_0a_{0_0}^0t_2\mathbf{p}_t^2] + \\ + [-(a_{0_1}^1\xi_1a_{0_1}^1 + a_{0_0}^0\xi_0a_{0_0}^0)\Delta t_1\mathbf{p}_{\Delta t}^1 - a_{0_0}^0\xi_0a_{0_0}^0\Delta t_2\mathbf{p}_{\Delta t}^2]; \\ e_{01}t_1\mathbf{p}_t^1 - e_0t_2\mathbf{p}_t^2 + (-a_{0_1}^1\xi_1a_{0_1}^1 + a_{0_0}^0\xi_0a_{0_0}^0)t_1\mathbf{p}_t^1 + a_{0_0}^0\xi_0a_{0_0}^0t_2\mathbf{p}_t^2 \leq \\ \leq \frac{e_{01}\Delta t_1\mathbf{p}_{\Delta t}^1 + e_0\Delta t_2\mathbf{p}_{\Delta t}^2}{2} + \frac{-(a_{0_1}^1\xi_1a_{0_1}^1 + a_{0_0}^0\xi_0a_{0_0}^0)\Delta t_1\mathbf{p}_{\Delta t}^1 - a_{0_0}^0\xi_0a_{0_0}^0\Delta t_2\mathbf{p}_{\Delta t}^2}{2} \quad \text{when} \\ \left(1 + \frac{\omega}{2}\right)[e_{01}\Delta t_1\mathbf{p}_{\Delta t}^1 + e_0\Delta t_2\mathbf{p}_{\Delta t}^2] + \left(1 + \frac{\omega}{2}\right)[-(a_{0_1}^1\xi_1a_{0_1}^1 + a_{0_0}^0\xi_0a_{0_0}^0)\Delta t_1\mathbf{p}_{\Delta t}^1 - a_{0_0}^0\xi_0a_{0_0}^0\Delta t_2\mathbf{p}_{\Delta t}^2]; \\ \frac{e_{01}\Delta t_1\mathbf{p}_{\Delta t}^1 + e_0\Delta t_2\mathbf{p}_{\Delta t}^2}{2} + \frac{-(a_{0_1}^1\xi_1a_{0_1}^1 + a_{0_0}^0\xi_0a_{0_0}^0)\Delta t_1\mathbf{p}_{\Delta t}^1 - a_{0_0}^0\xi_0a_{0_0}^0\Delta t_2\mathbf{p}_{\Delta t}^2}{2} \leq \\ \leq e_{01}t_1\mathbf{p}_t^1 - e_0t_2\mathbf{p}_t^2 + (-a_{0_1}^1\xi_1a_{0_1}^1 + a_{0_0}^0\xi_0a_{0_0}^0)t_1\mathbf{p}_t^1 + a_{0_0}^0\xi_0a_{0_0}^0t_2\mathbf{p}_t^2 \quad \text{when} \\ -\omega[e_{01}t_1\mathbf{p}_t^1 - e_0t_2\mathbf{p}_t^2] + [e_{01}\Delta t_1\mathbf{p}_{\Delta t}^1 + e_0\Delta t_2\mathbf{p}_{\Delta t}^2] - \omega[-(a_{0_1}^1\xi_1a_{0_1}^1 + a_{0_0}^0\xi_0a_{0_0}^0)t_1\mathbf{p}_t^1 + a_{0_0}^0\xi_0a_{0_0}^0t_2\mathbf{p}_t^2] + \\ + [-(a_{0_1}^1\xi_1a_{0_1}^1 + a_{0_0}^0\xi_0a_{0_0}^0)\Delta t_1\mathbf{p}_{\Delta t}^1 - a_{0_0}^0\xi_0a_{0_0}^0\Delta t_2\mathbf{p}_{\Delta t}^2]. \end{array} \right. \quad (43)$$

Auxiliary vectors are entered here:

$$p_t^1 = \begin{pmatrix} C_{P_x^1}t_1^{x_{P_x^1}-1} S_1^{y_{P_x^1}} V_1^{z_{P_x^1}} \\ C_{P_y^1}t_1^{x_{P_y^1}-1} S_1^{y_{P_y^1}} V_1^{z_{P_y^1}} \\ C_{P_z^1}t_1^{x_{P_z^1}-1} S_1^{y_{P_z^1}} V_1^{z_{P_z^1}} \end{pmatrix} \quad p_t^2 = \begin{pmatrix} C_{P_y^2}t_2^{x_{P_y^2}-1} S_2^{y_{P_y^2}} V_2^{z_{P_y^2}} \\ C_{P_x^2}t_2^{x_{P_x^2}-1} S_2^{y_{P_x^2}} V_2^{z_{P_x^2}} \\ C_{P_z^2}t_2^{x_{P_z^2}-1} S_2^{y_{P_z^2}} V_2^{z_{P_z^2}} \end{pmatrix} \quad (44)$$

$$p_{\Delta t}^1 = \begin{pmatrix} x_{P_x^1}t_1^{x_{P_x^1}-1} C_{P_x^1} S_1^{y_{P_x^1}} V_1^{z_{P_x^1}} \\ x_{P_y^1}t_1^{x_{P_y^1}-1} C_{P_y^1} S_1^{y_{P_y^1}} V_1^{z_{P_y^1}} \\ x_{P_z^1}t_1^{x_{P_z^1}-1} C_{P_z^1} S_1^{y_{P_z^1}} V_1^{z_{P_z^1}} \end{pmatrix} \quad p_{\Delta t}^2 = \begin{pmatrix} x_{P_y^2}C_{P_y^2}t_2^{x_{P_y^2}-1} S_2^{y_{P_y^2}} V_2^{z_{P_y^2}} \\ x_{P_x^2}C_{P_x^2}t_2^{x_{P_x^2}-1} S_2^{y_{P_x^2}} V_2^{z_{P_x^2}} \\ x_{P_z^2}C_{P_z^2}t_2^{x_{P_z^2}-1} S_2^{y_{P_z^2}} V_2^{z_{P_z^2}} \end{pmatrix} \quad (45)$$

p_t vector characterises the degree of influence of the cutting depth t , vector $p_{\Delta t}$ - the degree of influence of fluctuations in stock allowance Δt , $\omega = \varepsilon + \nu$ - values of the total scatter of the properties of the technological system. The cutting force, as a function of the parameter t , is determined by a well-known formula $p_i = c_i t^{x_i} s^{y_i} v^{z_i}$ $i = x; y; z$.

The model of the scattering field of dimensions performed in the opposite adjustment from the cross carriage is similar:

$$\Delta w_2 = \begin{cases} \left[\begin{aligned} &e_{02}t_2p_t^2 - e_0t_1p_t^1 + (-a_{02}^2\xi_2a_{02}^2 + a_{00}^0\xi_0a_{00}^0)t_2p_t^2 + a_{00}^0\xi_0a_{00}^0t_1p_t^1 \leq \\ &\leq -\frac{e_{02}\Delta t_2p_{\Delta t}^2 + e_0\Delta t_1p_{\Delta t}^1}{2} + \left(-\frac{(a_{02}^2\xi_2a_{02}^2 + a_{00}^0\xi_0a_{00}^0)\Delta t_2p_{\Delta t}^2 - a_{00}^0\xi_0a_{00}^0\Delta t_1p_{\Delta t}^1}{2}\right) \text{ when} \\ &\omega[e_{02}t_1p_t^1 - e_0t_1p_t^1] + [e_{02}\Delta t_2p_{\Delta t}^2 + e_0\Delta t_1p_{\Delta t}^1] + \omega[-(a_{02}^2\xi_2a_{02}^2 + a_{00}^0\xi_0a_{00}^0)t_2p_t^2 + a_{00}^0\xi_0a_{00}^0t_1p_t^1] + \\ &+ [-(a_{02}^2\xi_2a_{02}^2 + a_{00}^0\xi_0a_{00}^0)\Delta t_2p_{\Delta t}^2 - a_{00}^0\xi_0a_{00}^0\Delta t_1p_{\Delta t}^1]; \\ &e_{02}t_2p_t^2 - e_0t_1p_t^1 + (-a_{02}^2\xi_2a_{02}^2 + a_{00}^0\xi_0a_{00}^0)t_2p_t^2 + a_{00}^0\xi_0a_{00}^0t_1p_t^1 \leq \\ &\leq \frac{e_{02}\Delta t_2p_{\Delta t}^2 + e_0\Delta t_1p_{\Delta t}^1}{2} + \frac{-(a_{02}^2\xi_2a_{02}^2 + a_{00}^0\xi_0a_{00}^0)\Delta t_2p_{\Delta t}^2 - a_{00}^0\xi_0a_{00}^0\Delta t_1p_{\Delta t}^1}{2} \text{ when} \end{aligned} \right. \\ \left(1 + \frac{\omega}{2}\right)[e_{02}\Delta t_2p_{\Delta t}^2 + e_0\Delta t_1p_{\Delta t}^1] + \left(1 + \frac{\omega}{2}\right)[-(a_{02}^2\xi_2a_{02}^2 + a_{00}^0\xi_0a_{00}^0)\Delta t_2p_{\Delta t}^2 - a_{00}^0\xi_0a_{00}^0\Delta t_1p_{\Delta t}^1]; \\ \frac{e_{02}\Delta t_2p_{\Delta t}^2 + e_0\Delta t_1p_{\Delta t}^1}{2} + \frac{-(a_{02}^2\xi_2a_{02}^2 + a_{00}^0\xi_0a_{00}^0)\Delta t_2p_{\Delta t}^2 - a_{00}^0\xi_0a_{00}^0\Delta t_1p_{\Delta t}^1}{2} \leq \\ \leq e_{02}t_2p_t^2 - e_0t_1p_t^1 + (-a_{02}^2\xi_2a_{02}^2 + a_{00}^0\xi_0a_{00}^0)t_2p_t^2 + a_{00}^0\xi_0a_{00}^0t_1p_t^1 \text{ when} \\ -\omega[e_{02}t_2p_t^2 - e_0t_1p_t^1] + [e_{02}\Delta t_2p_{\Delta t}^2 + e_0\Delta t_1p_{\Delta t}^1] - \omega[-(a_{02}^2\xi_2a_{02}^2 + a_{00}^0\xi_0a_{00}^0)t_2p_t^2 + a_{00}^0\xi_0a_{00}^0t_1p_t^1] + \\ + [-(a_{02}^2\xi_2a_{02}^2 + a_{00}^0\xi_0a_{00}^0)\Delta t_2p_{\Delta t}^2 - a_{00}^0\xi_0a_{00}^0\Delta t_1p_{\Delta t}^1]. \end{cases} \quad (46)$$

In the non-opposed adjustment [23, 24] there is no counteraction of cutting forces. Therefore, the distortion scattering interval has a unique position - positive. The maximum is achieved with the largest allowances on both carriages, the maximum strength of the workpiece and the minimum compliance of the technological system, the minimum - in the opposite situation. As a result, for scattering fields of the dimensions performed in non-opposed adjustment, we obtain for longitudinal and cross carriages, respectively:

$$\Delta w_1 = \omega[e_{01}t_1p_t^1 + e_0t_2p_t^2] + [e_{01}\Delta t_1p_{\Delta t}^1 + e_0\Delta t_2p_{\Delta t}^2] + \omega[-(a_{01}^1\xi_1a_{01}^1 + a_{00}^0\xi_0a_{00}^0)t_1p_t^1 - a_{00}^0\xi_0a_{00}^0t_2p_t^2] + \quad (47)$$

$$+ [-(a_{01}^1\xi_1a_{01}^1 + a_{00}^0\xi_0a_{00}^0)\Delta t_1p_{\Delta t}^1 - a_{00}^0\xi_0a_{00}^0\Delta t_2p_{\Delta t}^2];$$

$$\Delta w_2 = \omega[e_{02}t_2p_t^2 + e^0t_1p_t^1] + [e_{02}\Delta t_2p_{\Delta t}^2 + e_0\Delta t_1p_{\Delta t}^1] + \omega[-(a_{02}^2\xi_2a_{02}^2 + a_{00}^0\xi_0a_{00}^0)t_2p_t^2 - a_{00}^0\xi_0a_{00}^0t_1p_t^1] + \quad (48)$$

$$+ [-(a_{02}^2\xi_2a_{02}^2 + a_{00}^0\xi_0a_{00}^0)\Delta t_2p_{\Delta t}^2 - a_{00}^0\xi_0a_{00}^0\Delta t_1p_{\Delta t}^1].$$

The vast majority of real multi-tool adjustments do not have such uniformity in the direction of cutting forces [23, 24]. Therefore, for adjustments that are inhomogeneous in direction, there is no single scheme for calculating scattering fields. The scheme for calculating the scattering field is determined separately for each coordinate direction, since one adjustment in the direction of one-run size can be opposite, and in the direction of another run size it can be non-opposite. If the adjustment of the considered direction is opposite, model (43) and (46) applied, but only a part of it in the direction of the considered size. For the non-opposed model, (47) and (48) applied, also only its part in the direction of the size under consideration.

By using two special models where (43) and (46) for opposed adjustments and (47) and (48) for non-opposed adjustments and the principle of the systematics of heterogeneous adjustments in the directions of executed sizes, it is possible to determine the scattering fields for the entire class of double-carriage deployed adjustments.

EXPERIMENTAL DETERMINATION OF ELEMENTS COMPLIANCE FOR A TECHNOLOGICAL SYSTEM.

The experiment involved measuring static compliance. Machine nodes were loaded with forces in axial directions, after which displacements in these and other directions of the technological system were determined (Figure 2). The obtained values made it possible to characterise the compliance of the technological system in the corresponding axial directions. To determine the angular compliance, the loading was performed by the moment of forces, and the angular displacements were determined by the linear displacement of two points in one plane (see Figure 2). As already mentioned, under the action of cutting forces, the nodes of the machine receive elastic displacements of two types, namely along the coordinate axes and angular, around the corresponding axes.

Determination of Compliance along with Coordinate Axes and Angular Compliance of Subsystems

Measurements were carried out on a CNC lathe INDEX V 160. The equipment consists of force measurement sensors (Kraftmessung–Kraftmessquarz Kistler Typ 9102 vorgespannt), a loading amplifier (Ladungsverstaerker Kistler Typ 5004), displacement measurement (Wegsensoren Solartron Typ AX/1/SH), an amplifier of measurement results (Messverstaerker HBM Typ MGCplus, Empfindlichkeit 100 $\frac{\mu m}{V}$ oder 10 $\frac{\mu m}{V}$), a signal receiver (Signalaufnahme National Instruments High Speed USD Carrier Typ Ni USD 9162, National Instruments Messkarte Typ Ni 9215, Filter : KEMO Typ VBF 8; Lowpass 10 Hz DC), and a laptop computer (Laptop HP Compaq nx 8220, Software : Ni LabView).

Measurement Scheme

The measurement stand for compliance of subsystems 0 and 1 is shown in Figure 2. To determine the corresponding compliance in the directions, loading was carried out by sequential force, after which the displacements in these and other directions of the technological system were determined (Figure 2). Loading and unloading of the elements of the system occurred gradually. The presence of joints and friction in technological system elements cause mismatch of the load and unload curves.

The experiments result to determine the matrix of static compliance for plane-parallel movements of subsystems 1 and 0 (in Figure 2) is presented in Figure 3 and 4. Figure 3 and 4 give the regression equation and reliability. Table 1 and 3 show the results of experiments to determine complex compliance in respective directions.

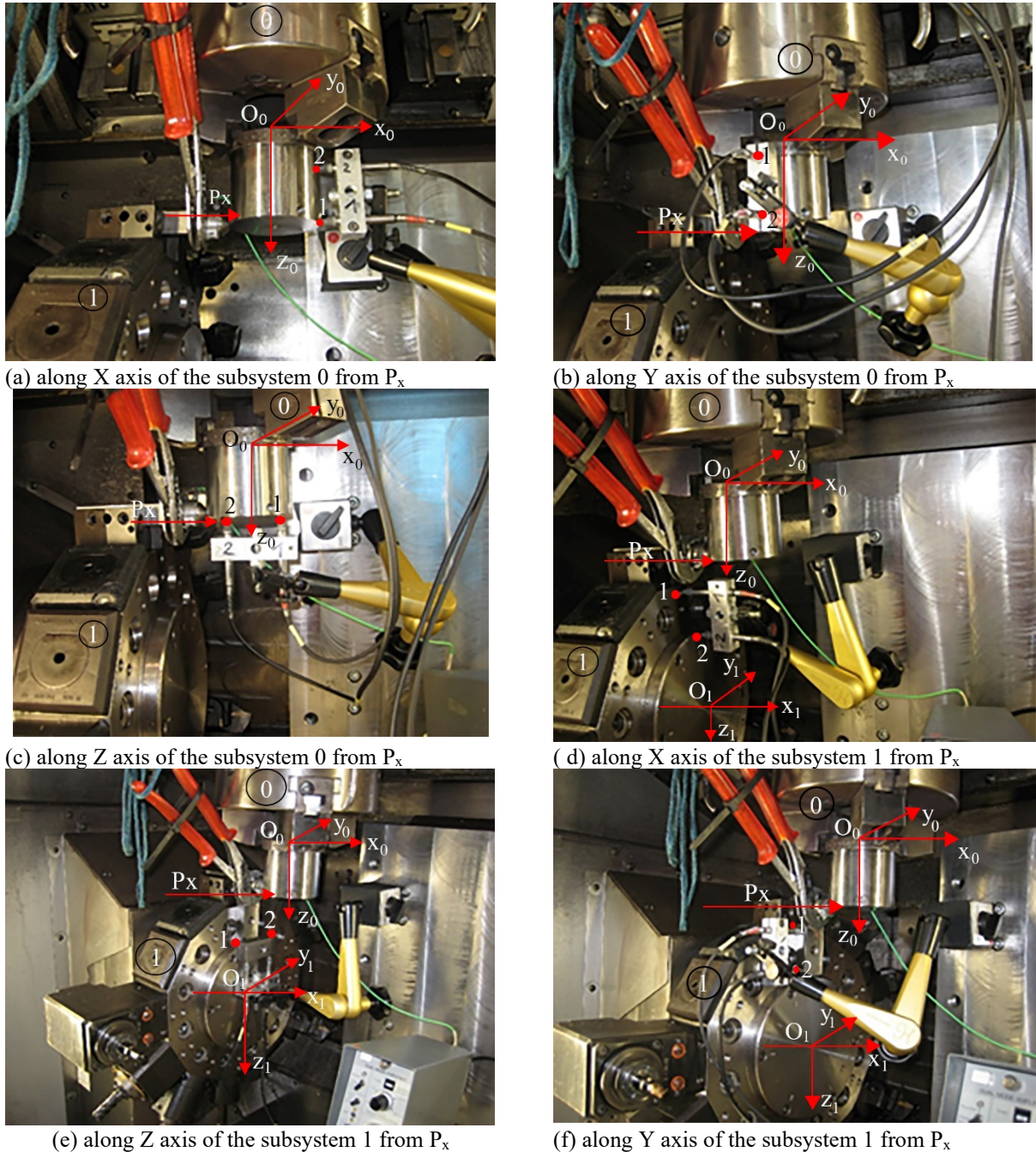


Figure 2. A stand for conducting an experiment to determine the complex compliance of subsystems 0 and 1.

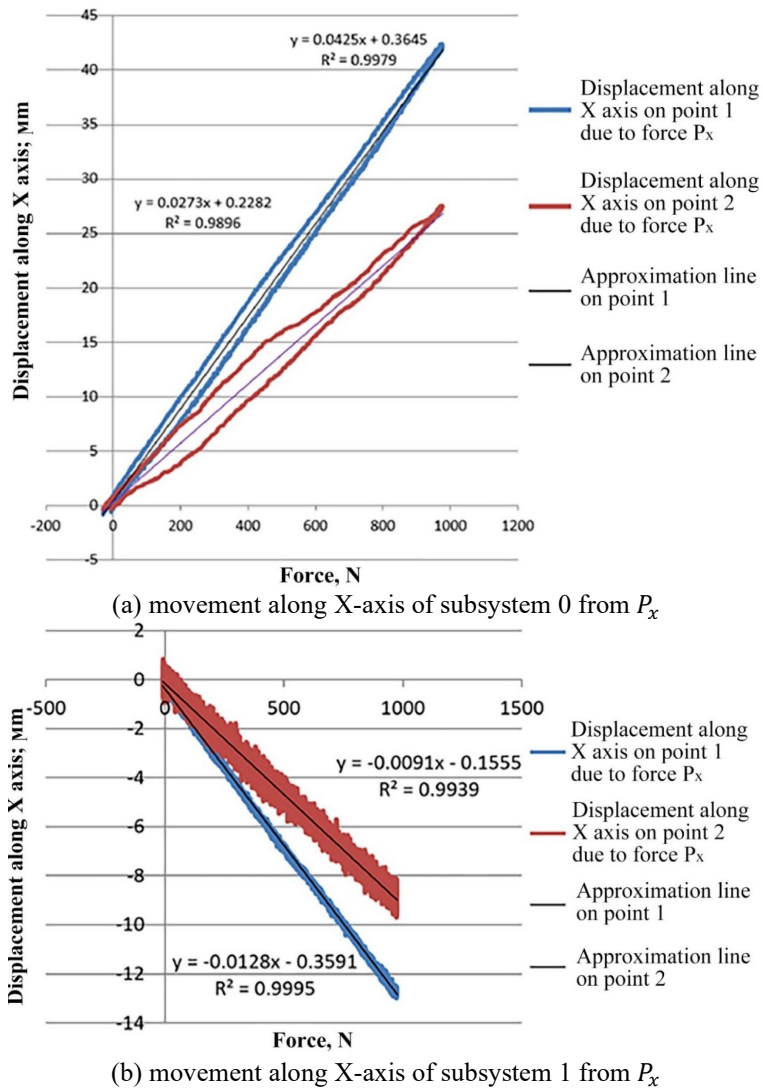
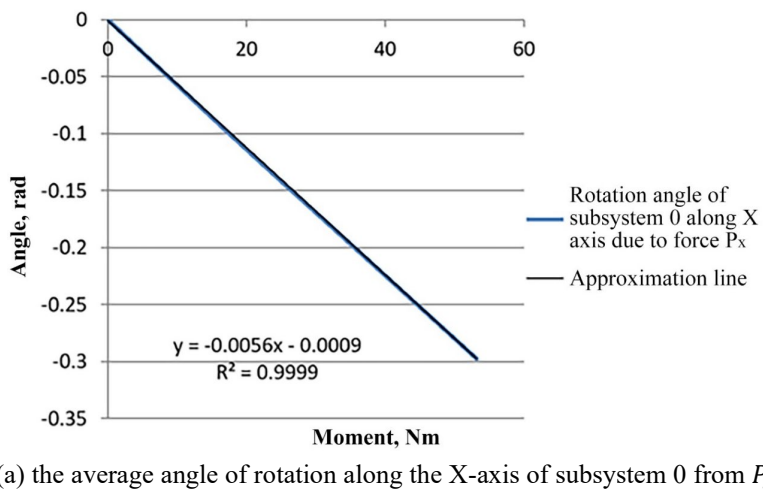
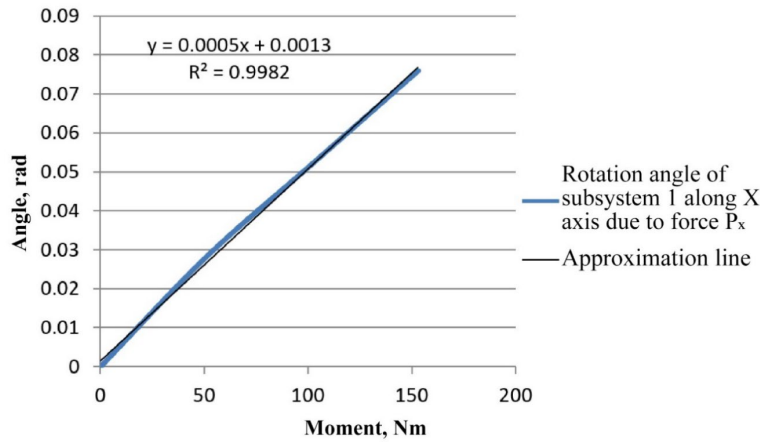


Figure 3. Fragments of experiment results to determine the coordinate matrix and the angular matrix ξ of compliance of subsystem 0 and 1.





(b) the average angle of rotation along X-axis of subsystem 1 from P_x

Figure 4. Fragments of experiments results to determine the angular matrix ξ of compliance of subsystem 0 and 1.

Table 1. Elements of the matrix of static e compliance for plane-parallel movements of subsystems.

	Compliance	Value (mkm/N)
Subsystem 0:	e_{xx}^0 - compliance in direction of X axis due to force P_x ;	0.0425
	e_{xy}^0 - compliance in direction of X axis due to force P_y ;	-0.0063
	e_{xz}^0 - compliance in direction of X axis due to force P_z ;	-0.0047
	e_{yx}^0 - compliance in direction of Y axis due to force P_x ;	0.0009
	e_{yy}^0 - compliance in direction of Y axis due to force P_y ;	0.0311
	e_{yz}^0 - compliance in direction of Y axis due to force P_z ;	-0.002
	e_{zx}^0 - compliance in direction of Z axis due to force P_x ;	-0.0105
	e_{zy}^0 - compliance in direction of Z axis due to force P_y ;	0.0054
	e_{zz}^0 - compliance in direction of Z axis due to force P_z ;	-0.011
Subsystem 1:	e_{xx}^1 - compliance in direction of X axis due to force P_x ;	-0.0128
	e_{xy}^1 - compliance in direction of X axis due to force P_y ;	-0.0033
	e_{xz}^1 - compliance in direction of X axis due to force P_z ;	0.001
	e_{yx}^1 - compliance in direction of Y axis due to force P_x ;	0.0026
	e_{yy}^1 - compliance in direction of Y axis due to force P_y ;	0.0072
	e_{yz}^1 - compliance in direction of Y axis due to force P_z ;	0.0032
	e_{zx}^1 - compliance in direction of Z axis due to force P_x ;	-0.0046
	e_{zy}^1 - compliance in direction of Z axis due to force P_y ;	0.0029
	e_{zz}^1 - compliance in direction of Z axis due to force P_z ;	0.007

Thus, we have identified the elements of elasticity coordinate matrix, e , that characterise the elasticity of technological system for each subsystem, the elasticity of the subsystems on the coordinate axes and their interaction. It should be noted that the directions of the X, Y, Z axes of the technological system shown in Table 1 correspond to the directions on the X, Y, Z axes shown in the mathematical models in the form of $X \Rightarrow Z, Y \Rightarrow X, Z \Rightarrow Y$. During the experiments, directions of the coordinate axes of the coordinate system of the applied machine were used. As can be seen from the table, the values of the elements of the coordinate matrix e_{xx}^0 (diametrical), e_{yy}^0 (circumference), e_{zz}^0 (length) of the elasticity of the subsystem 0 and the elements of the coordinate matrix e_{xx}^1 (diametrical), e_{yy}^1 (circumference), e_{zz}^1 (length) of the elasticity of the subsystem 1 are higher, i.e. their stiffness is lower. Value of element e_{xy}^0 is equal to 14,82% of e_{xx}^0 , value of e_{xz}^0 is equal to 11,06% of e_{xx}^0 . Similarly, the value of element e_{yx}^0 is equal to 2.89% of e_{yy}^0 , the value of element e_{yz}^0 is equal to 6.43% of e_{yy}^0 , the value of element e_{zx}^0 is equal to 95.45% of e_{zz}^0 , and the value of element e_{zy}^0 is equal to 49,09% of e_{zz}^0 . On the other hand, 79.44% of the elasticity in the general direction is in the share of e_{xx}^0 , 11.78% is in the share of e_{xy}^0 and 8.78% is in the share of e_{xz}^0 . Similarly, 91.47% of the elasticity in the general direction is in the share of e_{yy}^0 , 5.88% is in the share of e_{yz}^0 and 2.65% is in the share of e_{yx}^0 , as well as, 40.9% of the elasticity in the general direction is in the share of e_{zz}^0 , 39.03% is in the share of e_{zy}^0 and 20.07% is in the share of e_{zx}^0 . In the same way, the following considerations can be made for subsystem 1. Value of e_{xy}^1 is equal to 25,78% of e_{xx}^1 , value of e_{xz}^1 is equal to 7.81% of e_{xx}^1 . Similarly, value of e_{yx}^1 is equal to 36.11% of e_{yy}^1 , value of e_{yz}^1 is equal to 44.44% of e_{yy}^1 , value of e_{zx}^1 is equal to 65.71% of e_{zz}^1 and value of e_{zy}^1 is equal to 41.43% of e_{zz}^1 . On the other hand, 74.85% of the elasticity in the general direction is in the share of e_{xx}^1 , 19.30% is in the share of e_{xy}^1 and 5.85% is in the share of e_{xz}^1 . Similarly, 55.38% of the elasticity in the general direction is in the share of e_{yy}^1 , 24.62% is in the share of e_{yz}^1 and 20% is in the share of e_{yx}^1 , as well as, 48.28% of the elasticity in the general direction is in the share of e_{zz}^1 , 31.72% is in the share of e_{zx}^1 and 20% is in the share of e_{zy}^1 . Here, the following summary can be drawn about the elasticity of the 0 subsystem as a result of measurements:

Insufficient static elasticity (stiffness) is observed in both directions of the impact force of loading (in the direction of the X and Y axes), but the elasticity in the Z-axis is sufficient:

$$\begin{aligned} (e_{xx}^0 &= 0,0425 \frac{mkm}{N} \quad (j_{xx}^0 = 23,53 \frac{N}{mkm}); \\ e_{yy}^0 &= 0,0311 \frac{mkm}{N} \quad (j_{yy}^0 = 32,15 \frac{N}{mkm}); \\ e_{zz}^0 &= -0,011 \frac{mkm}{N} \quad (j_{zz}^0 = -90,91 \frac{N}{mkm})). \end{aligned}$$

The interaction of elasticity is felt (deformations, the effect of the force in the perpendicular directions):

$$\begin{aligned} (e_{xy}^0 &= -0,0063 \frac{mkm}{N} \quad (j_{xx}^0 = -158,73 \frac{N}{mkm}); \\ e_{xz}^0 &= 0,0047 \frac{mkm}{N} \quad (j_{xz}^0 = 212,77 \frac{N}{mkm}); \\ e_{yz}^0 &= -0,002 \frac{mkm}{N} \quad (j_{yz}^0 = 500 \frac{N}{mkm}); \\ e_{zy}^0 &= 0,0054 \frac{mkm}{N} \quad (j_{zy}^0 = 185,19 \frac{N}{mkm}); \\ e_{zx}^0 &= -0,0105 \frac{mkm}{N} \quad (j_{zx}^0 = -95,24 \frac{mkm}{N})). \end{aligned}$$

The interaction of elasticity is felt extremely weak in only one direction (deformations, the effect of force in the perpendicular directions):

$$(e_{yx}^0 = -0,0009 \frac{mkm}{N} \quad (j_{yx}^0 = 1111,11 \frac{N}{mkm} > 500 \frac{N}{mkm}))$$

Also, as a result of measurements, the following summary can be drawn regarding the elasticity of 1 subsystem:

Sufficient static elasticity (stiffness) is observed in all three directions of the impact force of loading (in the direction of the X, Y and Z axes):

$$\begin{aligned} (e_{xx}^1 &= -0,0128 \frac{mkm}{N} \quad (j_{xx}^1 = -78,13 \frac{N}{mkm}); \\ e_{yy}^1 &= 0,0072 \frac{mkm}{N} \quad (j_{yy}^1 = 138,89 \frac{N}{mkm}); \\ e_{zz}^1 &= 0,007 \frac{mkm}{N} \quad (j_{zz}^1 = 142,86 \frac{N}{mkm})). \end{aligned}$$

The interaction of elasticity is felt (deformations, the effect of force in the perpendicular directions):

$$\begin{aligned} (e_{xy}^1 &= -0,0033 \frac{mkm}{N} \quad (j_{xx}^1 = -303,03 \frac{N}{mkm}); \\ e_{yx}^1 &= 0,0026 \frac{mkm}{N} \quad (j_{yx}^1 = 384,62 \frac{N}{mkm}); \\ e_{yz}^1 &= 0,0032 \frac{mkm}{N} \quad (j_{yz}^1 = 312,5 \frac{N}{mkm}); \\ e_{zx}^1 &= -0,0046 \frac{mkm}{N} \quad (j_{zx}^1 = -217,39 \frac{N}{mkm}); \\ e_{zy}^1 &= 0,0029 \frac{mkm}{N} \quad (j_{zy}^1 = 344,83 \frac{N}{mkm})). \end{aligned}$$

The interaction of elasticity is felt extremely weak in only one direction (deformations, the effect of force in the perpendicular directions):

$$(e_{xz}^1 = 0,001 \frac{mkm}{N} \quad (j_{yx}^1 = 1000 \frac{N}{mkm} > 500 \frac{N}{mkm})).$$

Determination of Angular Compliance of Subsystems

In the passports for lathes, the angular compliance of subsystems 0 and 1 is not indicated. Therefore, along with the experimental method for determining plane-parallel displacements, the corresponding angular compliance method was developed in the work, and specific data were obtained for the INDEX V 160 CNC machine. Table 2 shows the values of the turning moment and rotation angles and the sequence of determining the angular compliance for subsystem 0 and 1. The angle of rotation θ of the subsystems is determined by the formula

$$\theta = \arctg(d_2 - d_1)/L \tag{49}$$

where d_1 is the elastic displacement of point 1, microns. d_2 - elastic displacement of point 2, microns. L - the distance between points 1 and 2, mm.

Table 2. Angular compliance of subsystem 0.

Moment, M (N·m)	Displacement, (mkm)		Distance between point 1 and 2 (mm)	Angle, in radian (10 ⁻³ rad)	Angular compliances (10 ⁻⁶ rad/N·m)
	Point 1	Point 2			
0	0	0	46.5	0	0
17.7	0.0131145	0.0084182	46.5	-0.100995699	-5,70597E-06
35.4	0.0258645	0.0166082	46.5	-0.199060212	-5,62317E-06
53.1	0.0386145	0.0247982	6.5	-0.297124722	-5,59557E-06

Table 3. Elements of the matrix of static ξ angular compliance of subsystem 0 and 1 of INDEX V 160 lathe with CNC.

Compliance	Value (rad/n*m)
Subsystem 0:	
ξ_{xx}^0 - compliance in direction of X axis due to force P_x	-5.6×10^{-6}
ξ_{xy}^0 - compliance in direction of X axis due to force P_y	1.1×10^{-6}
ξ_{xz}^0 - compliance in direction of X axis due to force P_z	2.7×10^{-6}
ξ_{yx}^0 - compliance in direction of Y axis due to force P_x	-0.5×10^{-6}
ξ_{yy}^0 - compliance in direction of Y axis due to force P_y	-3.6×10^{-6}
ξ_{yz}^0 - compliance in direction of Y axis due to force P_z	0.5×10^{-6}
ξ_{zx}^0 - compliance in direction of Z axis due to force P_x	2.6×10^{-6}
ξ_{zy}^0 - compliance in direction of Z axis due to force P_y	-3.3×10^{-6}
ξ_{zz}^0 - compliance in direction of Z axis due to force P_z	5.3×10^{-6}
Subsystem 1:	
ξ_{xx}^1 - compliance in direction of X axis due to force P_x	$0,5 \times 10^{-6}$
ξ_{xy}^1 - compliance in direction of X axis due to force P_y	$0,1 \times 10^{-6}$
ξ_{xz}^1 - compliance in direction of X axis due to force P_z	$0,5 \times 10^{-6}$
ξ_{yx}^1 - compliance in direction of Y axis due to force P_x	$0,03 \times 10^{-6}$
ξ_{yy}^1 - compliance in direction of Y axis due to force P_y	$-0,06 \times 10^{-6}$
ξ_{yz}^1 - compliance in direction of Y axis due to force P_z	$-0,4 \times 10^{-6}$
ξ_{zx}^1 - compliance in direction of Z axis due to force P_x	$0,06 \times 10^{-6}$
ξ_{zy}^1 - compliance in direction of Z axis due to force P_y	$0,4 \times 10^{-6}$
ξ_{zz}^1 - compliance in direction of Z axis due to force P_z	$-0,06 \times 10^{-6}$

Thus, we have identified the elements of the angular matrix of elasticity ξ of the subsystems of the technological system. As can be seen from the table, the elements ξ_{xx}^0 (diametrical), ξ_{yy}^0 (circular), ξ_{zz}^0 (length) of the angle matrix of elasticity of subsystem 0 and elements $\xi_{xx}^1, \xi_{xz}^1, \xi_{xy}^1, \xi_{yz}^1$, of coordinate matrix of elasticity of subsystem 1 are higher, i.e. their stiffness is lower. Value of element ξ_{xy}^0 is equal to 19,64% of ξ_{xx}^0 , value of ξ_{xz}^0 is equal to 48.21% of ξ_{xx}^0 . Similarly, the value of element ξ_{yx}^0 is equal to 13.89% of ξ_{yy}^0 , the value of element ξ_{yz}^0 is equal to 13.89% of ξ_{yy}^0 , the value of element ξ_{zx}^0 is equal to 49.06% of ξ_{zz}^0 , and the value of element ξ_{zy}^0 is equal to 62.26% of ξ_{zz}^0 . On the other hand, 59.57% of the elasticity in the general direction is in the share of ξ_{xx}^0 , 11.70% is in the share of ξ_{xy}^0 and 28.72% is in the share of ξ_{xz}^0 . Similarly, 78.26% of the elasticity in the general direction is in the share of ξ_{yy}^0 , 10.87% is in the share of ξ_{yz}^0 and 10.87% is in the share of ξ_{yx}^0 , as well as 47.3% of the elasticity in the general direction is in the share of ξ_{zz}^0 , 23.21% is in the share of ξ_{zx}^0 and 29.46% is in the share of ξ_{zy}^0 . In the same way, the following considerations can be made for subsystem 1. Value of ξ_{xy}^1 is equal to 20% of ξ_{xx}^1 , value of ξ_{xz}^1 is equal to 100% of ξ_{xx}^1 . Similarly, value of ξ_{yx}^1 is equal to 50% of ξ_{yy}^1 , value of ξ_{yz}^1 is equal to 66.67% of ξ_{yy}^1 , value of ξ_{zx}^1 is equal to 100% of ξ_{zz}^1 and value of ξ_{zy}^1 is equal to 66.67% of ξ_{zz}^1 . On the other hand, 45.45% of the elasticity in the general direction is in the share of ξ_{xx}^1 , 9.1% is in the share of ξ_{xy}^1 and 45.45%

is in the share of ξ_{xz}^1 . Similarly, 12.24% of the elasticity in the general direction is in the share of ξ_{yy}^1 , 81.63% is in the share of ξ_{yz}^1 and 6.13% is in the share of ξ_{yx}^1 , as well as, 37.50% of the elasticity in the general direction is in the share of ξ_{zz}^1 , 37.50% is in the share of ξ_{zx}^1 and 25% is in the share of ξ_{zy}^1 .

Thus, we experimentally determined the complex characteristics of the technological system. The proposed experimental method can be applied to other machines.

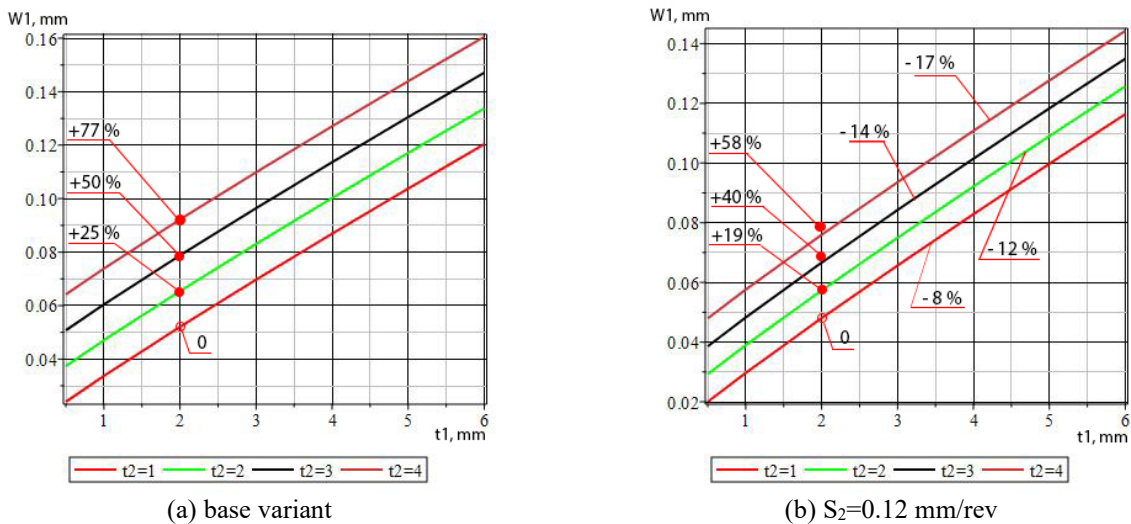
Theoretical Analysis of Machining Accuracy at Various Adjustments

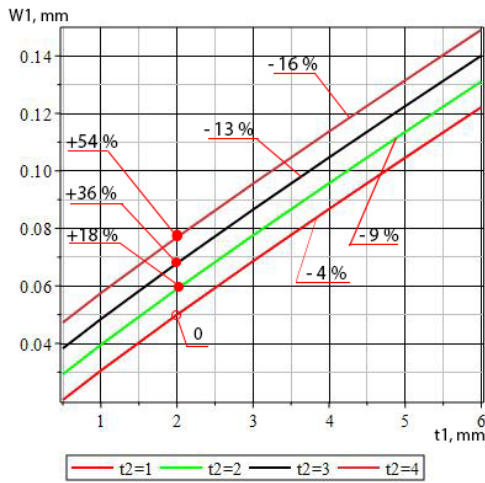
The proposed accuracy models take into account all the main factors of machining error:

- i. Machining allowance (t cutting depth);
- ii. Rigidity of the technological system $j_{xx}, j_{xy}, j_{xz}, j_{yx}, j_{yy}, j_{yz}, j_{zx}, j_{zy}, j_{zz}$;
- iii. Strength properties of the machined material (with the help of C_x, C_y, C_z)
- iv. Cutting conditions - feed S , cutting speed, group of the machined material and type of machining (with the help of $C_x, C_y, C_z, x_x, x_y, x_z$);
- v. Connecting vectors of points of application of forces P^1 and P^2 (with the help of matrices $a_{0_0}^0, a_{0_1}^1$ and $a_{0_2}^2$ - constituting the linking vectors of the P^1 and P^2 forces at the attached points relative to the base points of O_0, O_1 and O_2).

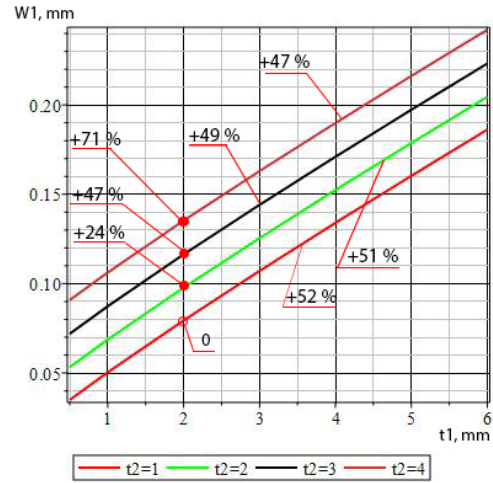
Such an abundance of factors taken into account turns the proposed models into a powerful tool for predicting and studying the accuracy of machining. To test the efficiency of the models, variants with different initial data were calculated that determine the sensitivity of the formula, that is, theoretical studies of the machining accuracy for various variants were performed. Let us show one of them as an example.

Figure 5 shows the technological and design factors influence on the distortion of the performed diametric size in dual-carriage adjustment. Here, in various versions, distorted values of the diametrical size were investigated, the basic version (Base version: two-carriage machining – longitudinal and cross carriages; workpiece – steel 45 (in GOST standard steel 45 is an analogy of AISI 1045 steel); cutting insert - CNMG 120408 P04 4225 CoroKey; dimensions of the workpiece: $D=L=74.9$ mm, workpiece accuracy – ITP_1I2, ITP_2I2 ; cutting speed – $V_1=V_2=200$ m/min.; feed $S_1=S_2=0,24$ mm/rev; the coordinates of the linking vectors of the points of application of the P^1 and P^2 forces relative to the base points of O_0 and O_1 : $X_0=74.9$ mm, $Y_0=37.45$ mm, $X_1=136$ mm, $Y_1=130$ mm. Changes for other options shown in the figure.) and base points were selected, and the operability of the developed models was accordingly checked. Figure 5(a) shows the degree of reflection effect on total displacements, depending on the technological and structural parameters of the subsystems in the formation of distortions for other allowance ($t_1=2$ mm and $t_2=2, 3, 4$ mm), taking in the basic version (0%) the longitudinal and cross carriage at allowance values of $t_1=2$ mm and $t_2=1$ mm. It should be noted that here the + sign indicates an increase, and the - sign indicates a decrease. Depending on various technological and design parameters, an increase in the distortion of the performed diametrical dimension in a two-carriage adjustment is between +18% and +98%, and other changeable options relative to the base case, is 20% to +428%.

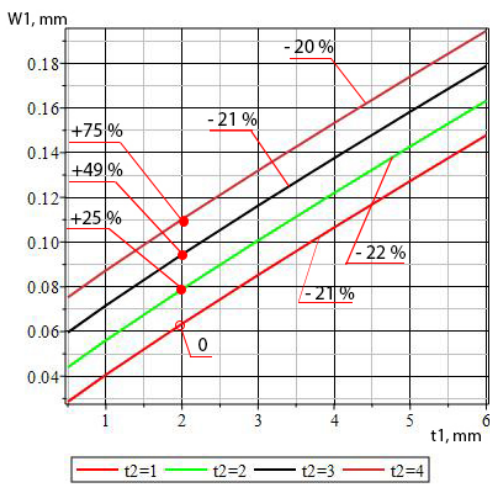




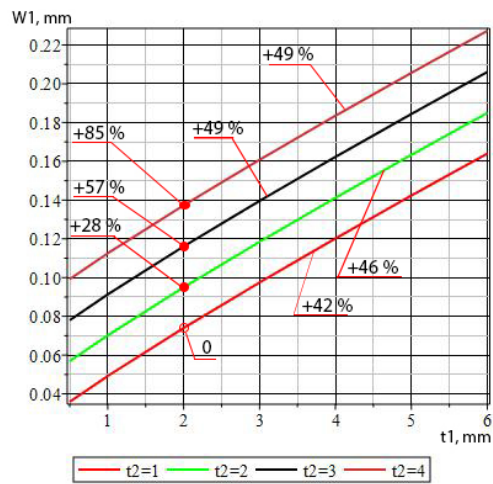
(c) $S_2=0.12$ mm/rev, $V_1=160$ m/min, $V_2=200$ m/min



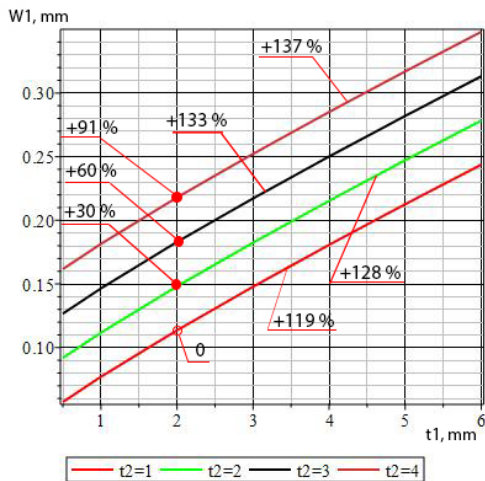
(d) $X_0=149.8$ mm, $Y_0=74.9$ mm, $X_1=272$ mm, $Y_1=260$ mm



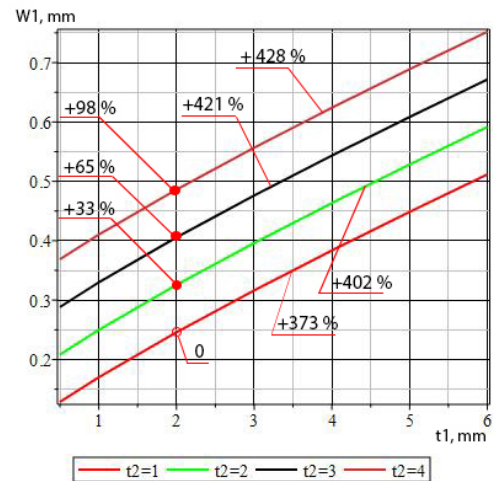
(e) $X_0=112.35$ mm, $Y_0=56.175$ mm, $X_1=204$ mm, $Y_1=195$ mm



(f) $X_0=149.8$ mm



(g) $X_0=224.7$ mm



(h) $X_0=374.5$ mm

Figure 5. The influence of technological and design factors on the value of distortion of the performed diametric size in two-carriage adjustment.

Thus, the models of dimensional accuracy developed for two-carriage adjustments reflect the influence of the main technological and design factors. For this reason, taking into account the required accuracy, they can be used during the design of operations.

CONCLUSION

The technological capabilities of CNC multi-purpose machines, possible options for the implementation of parallel multi-tool machining on them and the use of this type of equipment and tool adjustment at factories at present were analysed. It was revealed that many factories that have CNC multi-purpose machines use them at best for 50% of their technological capabilities. This situation has arisen due to the fact that there are no recommendations on the design and application of such adjustments. Therefore, the main prerequisite for solving this problem is to improve the theory of designing multi-tool machining, taking into account the capabilities of modern CNC machines. For this purpose, lattice-matrix models of precision multi-tool machining have been developed in order to fulfil the requirements of algorithmic uniformity of models and their structural transparency. An attempt was also made to obtain a generalised lattice-matrix model of machining accuracy for multi-carriage multi-tool adjustment. The use of lattice matrices greatly simplifies the error model of multi-tool machining and makes it extremely visual. On the need to take into account the angular displacements of the workpiece, in the case of machining parts with overall dimensions that significantly differ in different directions under the action of cutting forces, full-factor distortion models and scattering fields of the multi-tool machining dimensions performed on modern multi-purpose CNC lathe machines taking into account the compliance of the technological system according to all 6 degrees of freedom and thus allowing to take into account both plane-parallel and angular displacements in the technological system. Based on the developed models, it is possible to identify the degree of influence of complex of technological factors on the machining accuracy, including the structure of multi-tool setup, the deformation properties of the subsystems of the technological system, and cutting conditions. A methodology has been developed to determine the complex characteristics of technological system compliance;

- i. the matrix of coordinate compliance,
- ii. characterising the compliance of the subsystem along with the coordinate axes (their mutual influence and the matrix of angular compliance),
- iii. characterising the resistance to rotation around the coordinate axes and their interaction, and
- iv. the complex characteristic of the technological system compliance (experimentally determined) for each of the subsystems and the complex of two matrices (angular and plane parallel compliance of the technological system subsystems).

Considering both types of compliance, when setting up the machine, it is possible to take into account both plane-parallel and angular movements of the tool relative to the workpiece. The proposed experimental technique is applicable to other lathes too. The accuracy models in spatial adjustments make it possible to develop recommendations for designing adjustments of modern multi-purpose machines with CNC turning group, that is, to create CAD multi-tool machining. Thus, it is possible to achieve a number of ways to control multi-tool machining based on the developed accuracy models, including improving the structure of the multi-tool setup and calculating the limiting cutting conditions.

REFERENCES

- [1] Fesenko MA, Kondakov AI. Evaluation of productive capacity of cnc machining centers. *BMSTU Journal of Mechanical Engineering*. 2015; 667(10): 71-77.
- [2] Yusubov ND, Bagirova HM. Design of multi-tool machining in modern CNC multi-purpose lathes. In: 7th International scientific conference Information Technologies in Industry, Minsk, Belarus, pp. 176-178; 30-31 October, 2012.
- [3] Hirsch A. *Werkzeugmaschinen: Anforderungen, Auslegung, Ausführungsbeispiele*. Wiesbaden: Springer Vieweg; 2016.
- [4] Chuvakov AB. *Modern tendencies of development and foundations of effective operation of CNC machine tools*. Nizhny Novgorod: NSTU; 2013.
- [5] Bagrov BM, Kozlov AM. *Multi-purpose machines*. Lipetsk: LSTU; 2004.
- [6] Kalidasan R, Yatin M, Senthilvelan S, Sarma DK. Preliminary experimental investigation on multi-tool turning process. In: *Proceedings of the 5th International and 26th All India Manufacturing Technology, Design and Research Conference*, 12–14 December, IIT Guwahati, India, pp.50-1–50-5; 2014c.
- [7] Kalidasan R, Ramanuj V, Sarma DK, Senthilvelan S. Influence of cutting speed and offset distance over cutting tool vibration in multi-tool turning process. *Advanced Materials Research* 2014a; 984–985:100–105.
- [8] Kalidasan R, Yatin M, Sarma DK, Senthilvelan S. Effect of distance between two cutting tools over cutting forces and heat generation in multi-tool turning process. *Applied Mechanics and Materials*, 2014b; 592–594: 211–215.
- [9] Kalidasan R, Senthilvelan S, Dixit US, Vaibhav J. Double tool turning: machining accuracy, cutting tool wear and chip-morphology. *International Journal of Precision Technology* 2016; 6:142.
- [10] Benardos PG, Mosialos S, Vosniakos GC. Prediction of workpiece elastic deflections under cutting forces in turning. *Robotics and Computer Integrated Manufacturing* 2006; 22(5–6): 505–514.
- [11] Harik RF, Gong H, Bernard A. 5-axis flank milling: a state-of-the-art review. *Comput-Aided Design* 2013; 45(3):796–808.
- [12] Xu K, Wang J, Chu CH, Tang K. Cutting force and machine kinematics constrained cutter location planning for five-axis flank milling of ruled surfaces. *Journal of Computational Design and Engineering* 2017; 4(3):203–217
- [13] Wang C, Elber G. Multi-dimensional dynamic programming in ruled surface fitting. *Comput-Aided Design* 2014; 51:39-49.
- [14] Baskar N, Asokan P, Saravanan R, Prabhakaran G. Selection of optimal machining parameters for multi-tool milling operations using a memetic algorithm. *Journal of Materials processing technology* 2006; 174(1-3): 239-249.

- [15] Calleja A, Bo P, Gonzalez H, Bartoñ M, López de Lacalle LN. Highly accurate 5-axis flank CNC machining with conical tools. *The International Journal of Advanced Manufacturing Technology* 2018; 97: 1605-1615.
- [16] Shchurov IA, Nemitova EV, Shchurova AV, Ardashev DV. Metric buttress thread milling and turning on CNC machines. *International Journal of Automotive and Mechanical Engineering* 2018;15(2): 5146-5160.
- [17] Civcisa G. The relationship between advanced manufacturing technologies and ISO 9001 certified enterprises of mechanical engineering and metalworking in Latvia. *International Journal of Automotive and Mechanical Engineering* 2018; 15(3): 5625-5635.
- [18] Kumar R, Modi A, Panda A et al. Hard turning on JIS S45C structural steel: An experimental, modelling and optimisation approach. *International Journal of Automotive and Mechanical Engineering* 2019; 16(4): 7315-7340.
- [19] Sivareddy DV, Krishna P, Gopal A, Prithvi Raz C. Parameter optimisation in vibration assisted turning of Ti6Al4V alloy using ANOVA and Grey relational analysis. *International Journal of Automotive and Mechanical Engineering* 2018; 15(3): 5400-5420.
- [20] Gupta M, Kumar S. Optimisation of the material removal rate in turning of UD-GFRP using the particle swarm optimisation technique. *International Journal of Automotive and Mechanical Engineering* 2013; 8: 1226-1241.
- [21] Najiha MS, Rahman MM, Yusoff AR. Modeling of the end milling process for aluminum alloy AA6061T6 using HSS tool. *International Journal of Automotive and Mechanical Engineering* 2013; 8: 1140-1150.
- [22] Saha A. Empirical modelling of machining parameters for turning operations using multiobjective Taguchi method. *International Journal of Automotive and Mechanical Engineering* 2017; 14(3): 4448-4461
- [23] Yusubov ND. Matrix models of the accuracy in multitool two-support setup. *Russian Engineering Research* 2009; 29(3): 268-271.
- [24] Yusubov ND. Fundamentals of matrix theory of accuracy of multi-tool turning. (Principles and structure of the theory, design and management of multi-tool machining processes). Saarbrücken, Germany: LAMBERT Academic Publishing; 2013.
- [25] Yusubov ND. Multi-tool machining on automatic lathes (Matrix theory of multi-tool machining accuracy on modern CNC lathes). Saarbrücken, Germany: LAMBERT Academic Publishing; 2013.
- [26] Yusubov ND. Algorithmization of analytical model of dimensions stray field, executed in multi-tool multi-carriage adjustments. *Vestnik Mashinostroeniya*. 2008; 2: 54-56.
- [27] Koshin AA, Yusubov ND. Elements of matrix theory of multi-tool processing accuracy in three-dimensional setups. *Vestnik Mashinostroeniya*. 2013; 9: 13-17.
- [28] Yusubov ND. Matrix models of working accuracy at single-cutter turning. *Journal Tekhnologiya Mashinostroeniya*. 2009;1:41-45.
- [29] Pimenov DY, Guzeev VI, Koshin AA. Elastic displacement of a technological system in face milling with tool wear. *Russian Engineering Research*. 2011; 31(11): 1105-1109.
- [30] Brecher C, Epple A, Neues S, Fey M. Optimal process parameters for parallel turning operations on shared cutting surfaces. *International Journal of Machine Tools and Manufacture* 2015; 95: 13-19.
- [31] Budak E. Dynamics and stability of parallel turning operations. *CIRP Annals Manufacturing Technology* 2011; 60(1): 383–386.
- [32] Guzeev VI, Pimenov DY. Cutting force in face milling with tool wear. *Russian Engineering Research* 2011; 31(10): 989-993.
- [33] Pimenov DY, Guzeev VI, Mikolajczyk T, Patra K. A study of the influence of processing parameters and tool wear on elastic displacements of the technological system under face milling. *The International Journal of Advanced Manufacturing Technology* 2017; 92(9-12): 4473-4486.
- [34] Pimenov, Guzeev VI, Krolczyk G et al. Modeling flatness deviation in face milling considering angular movement of the machine tool system components and tool flank wear. *Precision Engineering* 2018; 54: 327-337.
- [35] Nguyen HT, Wang H, Hu SJ. High-definition metrology enabled surface variation control by reducing cutter-spindle deflection. In: 9th ASME International Manufacturing Science and Engineering Conference (MSEC2014), 2014: 4017.
- [36] Ozturk E, Comak A, Budak E. Tuning of tool dynamics for increased stability of parallel (simultaneous) turning processes. *Journal of Sound and Vibration* 2016; 360: 17-30.
- [37] Dyakonov AA, Kh. Nurkenov A, Shmidt IV et al. Static rigidity of numerically controlled lathes. *Russian Engineering Research* 2017; 37(7): 622-625.
- [38] Tyler CT, Troutman JR, Schmitz TL. A coupled dynamics, multiple degree of freedom process damping model, Part 1: Turning. *Precision Engineering* 2016; 46: 65-72.
- [39] Azvar M, Budak E. Multi-dimensional chatter stability for enhanced productivity in different parallel turning strategies. *International Journal of Machine Tools and Manufacture* 2017; 123: 116-128.
- [40] Takasugi K, Morimoto Y, Kaneko Y et al. Improvement of machining accuracy for 3D surface machining with CNC lathe. *Journal of Advanced Mechanical Design Systems and Manufacturing* 2018; 12(4): 18-00034.
- [41] Usubatov Ryspek, Zain ZM, Sin TC, Kapaeva S. Optimisation of multi-tool machining processes with simultaneous action. *The International Journal of Advanced Manufacturing Technology* 2018; 82: 1227–1239.
- [42] Xiong CH. An approach to error elimination for multi-axis CNC machining and robot manipulation. *Science in China Series E: Technological Sciences* 2007; 50: 560-574.